


Diploma Thesis

Medical Informatics
University of Heidelberg/Heilbronn University

Three Channel Dynamic Photometric Stereo

Michelle Beyeler

March 8th, 2011

First Reviewer: Prof. Dr. Thomas Wetter
Institute of Medical Informatics, University of Heidelberg

Second Reviewer: Chi-Hsien Chen, MD, PhD
Taipei Medical University, Wan Fang Hospital, Taipei, Taiwan

Universität Heidelberg
Hochschule Heilbronn
Medizinische Informatik

Studiengang Medizinische Informatik
Masterstudiengang Informationsmanagement in der Medizin

Michelle Beyeler ..... 165934 .....

(Name, Vorname) (Matrikelnummer)

Thema der Diplom-/Masterarbeit: .....

.....

Three Channel Dynamic Photometric Stereo

.....

Ich erkläre hiermit an Eides Statt, dass ich die vorliegende Arbeit selbstständig und ohne Benutzung anderer als der angegebenen Hilfsmittel angefertigt habe; die aus fremden Quellen (einschließlich elektronischer Quellen) direkt oder indirekt übernommenen Gedanken sind als solche kenntlich gemacht.
Bei der Auswahl und Auswertung des Materials sowie bei der Herstellung des Manuskripts habe ich Unterstützungsleistung von folgenden Personen erhalten:

.....

Prof. Dr. Thomas Wetter, Institute of Medical Informatics, University of Heidelberg

.....

Chi-Hsien Chen, MD, PhD, Taipei Medical University, Wan Fang Hospital, Taipei, Taiwan

.....

.....

Die Arbeit wurde bisher weder im Inland noch im Ausland in gleicher oder ähnlicher Form einer anderen Prüfungsbehörde vorgelegt und ist auch noch nicht veröffentlicht.

Biel (Switzerland), 2011-03-08 .....

(Ort, Datum) (Unterschrift)

Acknowledgement

First I want to thank Chi-Hsien Chen and Thomas Wetter for the support during my stay in Taipei. Chi-Hsien Chen gave me an important assistance before the trip with the administrative matters and a good start with the project, while Thomas Wetter established the contact to Chi-Hsien Chen and gave me a valuable support from Germany especially in difficult situations.

I also want to thank the Wan Fang Hospital and the Taipei Medical University for the great organization and the opportunity they gave me by cooperating with the University of Heidelberg. Thanks to Robert K.Tsui for his warm welcome at the Wan Fang Hospital.

Wolfram Schulze gave me a lot of practical inputs for starting my work and also backed me up together with Walter Schroeder from Germany, many thanks to them.

Particular and deep-hearted thanks go to Ashley Cheng for her never ending help in administrative matters, personal topics, Chinese translations, giving me tips for the Taiwanese life, for showing me the country's culture every day and for her sincere friendship. I would not forget what she has done for me.

Also, I want to thank all the colleagues of the rehabilitation department for the friendly cooperation and open-mindedness. Abener, Oliver, Chou, Wenyen, Pulong, Jeremy, Jo, Nicole, Monika, Kevin, Frank, Stacy were my friends during my stay, thanks to them for their friendship, the shared time and being patient when introducing me to the Taiwanese culture so well. Many thanks also to the teams of the 7-Eleven and the Starbucks Coffee at the Wan Fang Hospital for their warm and friendly welcome every day.

A very special "thank you" to Luzie Schreiter, my dear friend who shared a part of this trip with me and gave me many good memories to keep in mind. Thanks for being there and believing in me.

Also I'd like to thank Simon Pezold for proofreading this work so meticulously and giving me many valuable advices.

Special thanks to my mother, my sister and my friends in Switzerland and Germany for being there and believing in me before, during and after the trip in Taiwan. Particular thanks go also to Chris who supported me during the hard times from New York and just was there for me.

谢谢

Michelle Beyeler

“The man who removes a mountain begins by carrying away small stones.”

Chinese proverb

Content

Abstract

The use of three-dimensional (3D) surface and volume reconstruction is increasing in many medical fields. Compared to the wide-spread methods like computer tomography (CT) or magnetic resonance imaging (MRI), Photometric Stereo is an alternative for screening purposes which is cheaper and harmless for the patient.

Photometric stereo is based on the idea of “shape from shading” and is a method for 3D surface reconstruction of an object from its multiple images taken from a fixed viewpoint under different illumination directions.

This thesis presents a photometric stereo method based on the work of Schulze [*35*], who in turn extended the research of Schroeder et al. [33,34] In this approach, three different lightings are obtained by illuminating the object by three colored light sources (red, green and blue). A video of the subject is captured from the front, the back and the side. The single frames are then extracted from the video, which are used for the 3D reconstruction of the subject.

The aim of this work was to improve the presented method of Schulze with real patient subjects by getting a better sphere calibration and changing some parameters in the patient processing. As the graphical interface was implemented for persons with a technical background, it has been changed to become also more convenient to use for non-technically oriented staff.

Finally, the work analyzes the encountered problems during this task and presents some improvement measures for further work.

1. Introduction

1.1. Surface/Volume Reconstruction and Movement Analysis

The use of imaging processes is increasing constantly in many medical fields and for many purposes. In health care, the most known imaging techniques are computer tomography (CT), X-rays, magnetic resonance imaging (MRI) and ultrasound.

These methods are wide-spread as they provide important information about the patient's condition and are essential for making a reliable diagnosis. MRI and CT create a three-dimensional (3D) model of the human body, which helps medical professionals to extract important qualitative or quantitative data about the patient. The goal when reconstructing a body surface or volume is to get the depth of an image.

The 3D image techniques are utilized for external measurements of the body shape and volume. With the body shape, medical professionals can calculate the requirements of drug or radiotherapy dosages. It can be employed for evaluating skin damages in burn victims or other dermatology patients. The visualization of a patient's body can be helpful for diet or exercise programs as it reveals more details than a simple mirror in front of the person. Moreover, surgeons can use the 3D visualization to plan their surgical intervention. The 3D demonstration of the effects of a treatment or a cosmetic surgery on a model can be a possibility to improve the patient's understanding and therefore also the patient compliance. [25,40] Also, 3D surface reconstruction can be used in diabetic patients for calculating the proportion of visceral fat in the body.

Although these procedures are widely-used, they show some disadvantages. The methods consume a lot of time and memory as they have to calculate very complex algorithms. Also they are expensive, as they produce high material and personnel costs. Besides that, a lot of space is used for installing the machines, which is an important aspect for many hospitals. In addition, the methods can be harmful for patients when using radioactive or chemical substances and are therefore not suited for screening purposes.

These difficulties can be avoided when reconstructing surfaces and volumes with photometric methods which are presented in the following section.

1.2. Previous Work

Photometric Stereo has been introduced by Woodham in 1980 [*45*]. He proposed a method for recovering the surface of an object from its multiple images taken under different illumination directions by holding the viewing direction constant.

This idea has been picked up by a large number of studies since then, which improved and varied the method in several ways during the last 30 years.

While Woodham's technique was based on Lambertian surfaces, Nayar et al. [*26*] presented a photometric sampling method which identifies both Lambertian and specular reflections by using extended light sources.

In 1994, Hayakawa [*13*] introduced an uncalibrated photometric stereo approach. The object surface is recovered without knowing a priori the lighting conditions like the light source direction or intensity. Also, no assumption is made about the surface reflection. The method only assumes that

the object's surface is Lambertian. The surface normals are estimated from input images by Singular Value decomposition (SVD).

Christensen and Shapiro [*4*] suggested a shading function mapping the surface normals to the color space under a given illumination. Using a calibration sphere, they implemented lookup tables in order to represent the inverse shading function for a given image configuration.

A four-source photometric stereo approach has been proposed by Barsky and Petrou [*2*]. Their algorithm separates the local gradient information and Lambertian color and deals with the problem of shadows and highlights by pixel-wise estimating the color.

Based on the orientation-consistency, Hertzmann and Seitz's theory [*16*] is saying that two points with the same surface orientation have a similar appearance in an image. For each point on the target object, their method finds a matching point on the reference object. No calibration for the camera or the light sources is needed.

In 2007, Basri et al. [*3*] presented a photometric method with general, unknown lighting. They showed that images of Lambertian objects captured under unknown lighting can be represented by a lower dimensional linear set of images.

While a lot of photometric approaches are based on a single viewpoint, the technique of Hernandez et al [*14*] uses multiple viewpoints under varying lighting conditions. After recovering camera motion, the algorithm constructs the visual hull of a Lambertian object, which is sufficient to recover an unknown illumination direction and intensity of an image. With this information, a multiple view stereo scheme is then created.

Alldrin et al. [*1*] assumed that objects are made of different materials and restricted the reflectance function so that it is fulfilled for all observed physical properties of the different materials. This has been reached by reducing the domain of the bi-directional reflectance distribution function (BRDF) from a function of four variables to a function with two variables.

In order to avoid shadows or highlights falsifying results, Plata et. al. [*29*] extended the four-source photometric stereo approach and used albedo that is, reflectivity information, instead of RGB (red, green, blue) information. Spectral reflexions in single pixels were recovered from the albedo values. After recovering the surface shape, this spectral reflectance information is then added. This allows a simulation of a sample under any illumination direction and different spectral sources.

Hernandez and Vogiatzis [*15*] developed an algorithm in 2010 which reconstructs 3D objects from images using a pipeline of four building blocks, namely the camera calibration, the image segmentation, the photo-consistency estimation from images and the surface extraction from photo-consistency.

Zheng et al. [*48*] introduced in the same year a photometric approach using specularities, based on the main ideas of Hertzmann and Seitz [*16*] and Alldrin et al. [*1*] Every specular reflection is expressed by using fixed specular basis functions. There is no need that reference objects must be of the same appearance as the test objects.

1.3. Three Channel Dynamic Photometric Stereo

Photometric stereo is based on the idea of “shape from shading”. It is a method of recovering the surface of an object from its multiple images taken from a fixed viewpoint under different illumination directions.
The normals of the surface points are deduced from the intensity values obtained by the different lighting directions and then used to calculate the depth map by integrating the gradient field. The approach assumes Lambertian reflection (also see section 3.1.2), distant light sources and orthographic camera projection. Photometric stereo can be separated into static and dynamic photometric stereo. The static photometric stereo is often referred to as the conventional photometric stereo, meant to recover images from a static object or patient.
Photometric stereo techniques with two lights allow recovering two-dimensional objects as shown in Fig. 1.1 a):

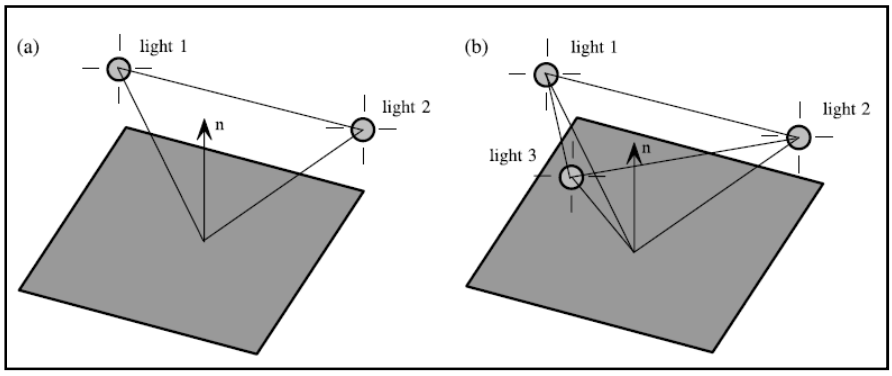

Fig. 1.1 Schema of 2D (a) and 3D (b) photometric stereo [*37*]

The component outside the plane is still indeterminate as it has two possible solutions. Therefore this approach is only working for two-dimensional, planar objects. For getting a single solution for the unknown third component, a third light source is needed (Fig. 1.1 b)).

Photometric stereo recovers 3D information from the surface, which is given in a three-component normal vector, representing the surface orientation of a surface point. This means that also three images will be needed to obtain the three normal components.

2. Motivation and Objective

2.1. Motivation

In the field of 3D surface reconstruction, a lot of methods have been developed in recent years. However, most of them are very expensive and time-consuming, and a few even harmful for patients when radioactive substances or chemicals are used. Besides that, the techniques have to be approved when they are used in the clinical field.

These are many reasons for developing a method which is cheaper and less harmful to the human body. Chen et al [*34*] presented a method in their work based on Photometric Stereo creating 3D models of patients, which was applicable on static objects.

He used the proposed method in the field of rehabilitation. However, the technique is also imaginable for Diabetes type 2 prevention by measuring the visceral fat volume in risk patients.

Schroeder and Schulze [34,35] continued this idea and implemented a method able to reconstruct a 3D model from a subject filmed in three views (back, front, side). The application is usable for moving patients, but the movements are restricted to be on the same plane. Thus, the 3D reconstruction is not working for rotations around the longitudinal axis. [*35*]

Although the method is working very well for a human dummy, Schulze showed that there is some improvement to do when using it with real patients.

2.2. Objective

This work was thought to go further with the work of Schroeder and Schulze [34,35] by improving the 3D reconstruction results in order to make the application usable with real patients. This should be realized with a better calibration and experiments conducted with real patients of different shape. Moreover, the graphical user interface should be improved and made more user-friendly also for non technically-oriented staff.

In this context, the central questions are:

- How can the system calibration be improved?
- Which parameters can be changed on the real patient subject to get a better 3D reconstruction?
- What makes the graphical user interface more user-friendly?

The application has been developed in order to be used in the clinic later. As many aspects have to be considered for this purpose, further project work is necessary. For this, the main question to be answered is:

- Which are the crucial points for further work and for eventually taking over of this project?

3. Materials and Methods

This chapter shows the physical and mathematical basics needed to understand the method presented in this work. However, not all fundamentals will be explained as this thesis is based on the results of Schroeder and Schulze [34,35] which gave an extensive introduction into the topic. Their works should be read if more technical details and explanations are required.

3.1. Physical and Mathematical Basics

3.1.1. Light and Color

Light is the electromagnetic radiation that can be detected by the human eye. The perceived color corresponds to the nature of the light reflected from the object. Visible light has a wavelength between 400 and 700 nm and this range is called the visible spectrum.

The retina at the back of the human eye contains two kinds of photo-sensitive cells: the rods and the cones. The **rods** are used for sensing the light intensity at low-light while the **cones** can discern colors and function best at bright light. The latter can be divided into three different types: short (S), medium (M) and long (L), all named after their sensitivity to short, medium and long light wavelengths. By assigning a number to each of these three cells illustrating the light intensity, we'll get a tri-component vector describing one specific color. The vector space built by all colors is called color model or color space. [6,30,41]

Two types of color models can be distinguished:

- the **additive color models**:
  the colors are created by combining light sources with different wavelengths and the convergence of the three primary colors produces white (Fig. 3.1, a))
- the **subtractive color models**:
  the colors are obtained by subtracting specific parts of a spectrum and the convergence of the three primary colors produces black (Fig. 3.1, b))

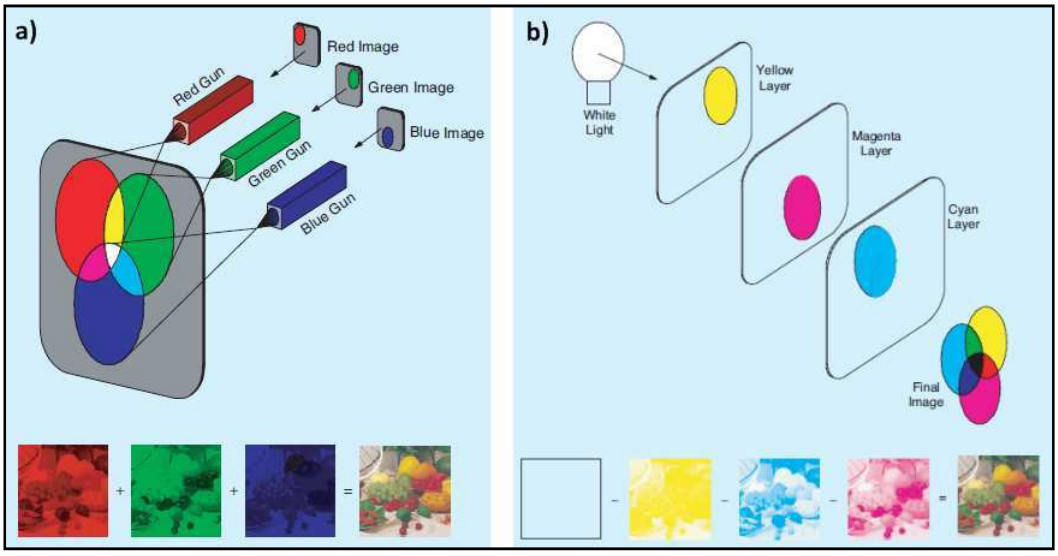

Fig. 3.1 Additive color systems (a) and subtractive color systems (b) [42]

The most known color system is **the RGB color space** based on the **trichromatic theory**. It is an additive model in which red, green and blue are combined in various ways to reproduce other colors. It can be represented by a three-dimensional, Cartesian coordinate system where every axis stays for one of the three colors (Fig. 3.2):

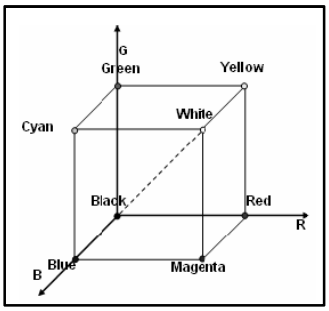

Fig. 3.2 The RGB cube [*10*]

Another representation of the trichromacy is given by the CIE color space introduced by the "Commission Internationale de l'Eclairage" (CIE) in 1931. It is described by the color intensity and two additional components x and y building a two-dimensional color space [*30*] as shown in Fig. 3.3:

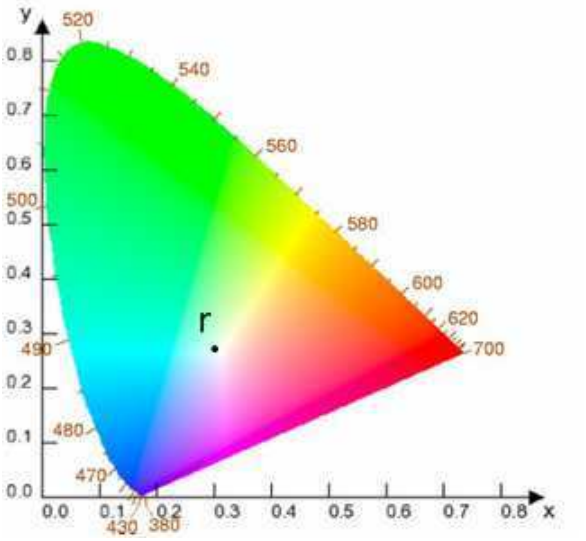

Fig. 3.3 CIE Chromaticity diagram (adapted from [50])

Every RGB value is linked to a x,y,z value based on the **tristimulus**:

$$x + y + z = 1 \tag{3.1}$$

This means that the values x, y and z are expressed as a proportion of a total:

$$x = \frac{x}{x + y + z} \qquad y = \frac{y}{x + y + z} \qquad z = \frac{z}{x + y + z} \tag{3.2}$$

In Fig. 3.3, the reference point r is the white point where the proportion of red, green and blue is the same, or in other words where $x = y = z$.

Another important color model is the **HSV (Hue, Saturation, Value) model** also known **as HSB (Hue, Saturation, Brightness) model**. It is a linear transformation of the RGB model and defines colors by three components: the **hue** which represents the dominant color type, the **saturation** indicating the intensity of the specific hue and the value standing for the color **brightness** (Fig. 3.4):

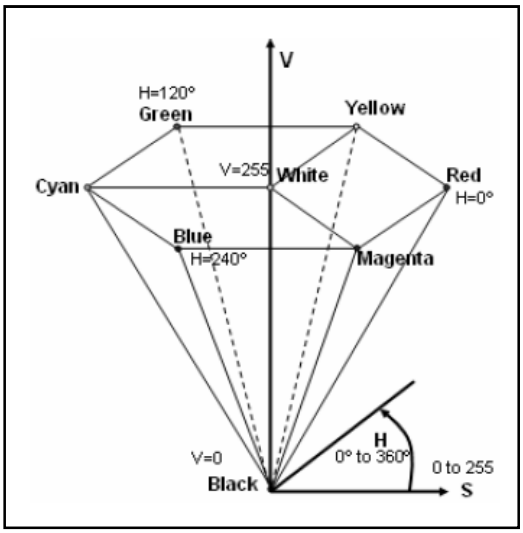

Fig. 3.4 The HSV-cone [*10*]

Finally, another important model is the **CMYK (Cyan, Magenta, Yellow, Key or Black) model**. As it is mainly used for printing purposes and not relevant for this work, it would not be explained in details here.

3.1.2. Reflection and the Lambertian Reflection Model

Two basic optical quantities for lighting intensities are radiance and irradiance. The **irradiance** represents the amount of incidence light falling on a surface for a given area and is used to measure the lighting intensity. On the other side, the **radiance** corresponds to the energy emitted by a unit area of an emitting surface in a given direction and is used to measure the lighting sources. It is the product of the scene irradiance and the reflectance. The **reflectance** in turn is represented by a function of the direction of the surface normal relative to the direction of the light source and the direction of the observer or in our case the camera.

The direction of a light ray after striking a medium will depend on the medium itself. A light ray will travel in a straight line in a homogeneous medium. When encountering another medium, it will change direction as a part of the incident light is reflected. Depending on the surface of the object, the reflection will be either specular or diffuse.

In the case of a smooth surface like a mirror, we are speaking of **specular reflection**. The angle between the incident ray and the normal (angle of incidence α) equals the angle between the normal and the reflected light ray (angle of reflection β), which is called the law of reflection (Fig. 3.5).

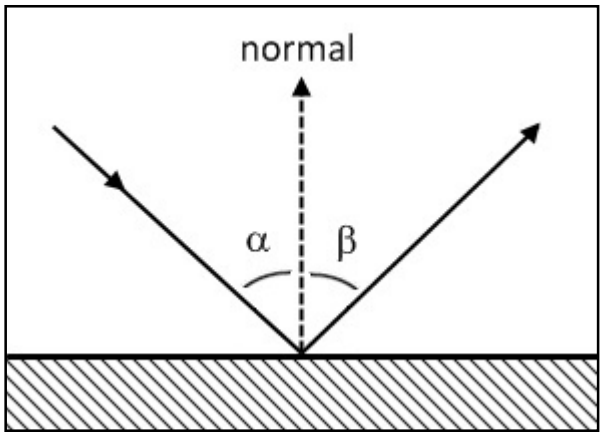

Fig. 3.5 Specular reflection: law of reflection

Thus, specular reflection changes with the viewing angle as the perceived reflected light will be different for each observation point and angle.

When a surface is rough, the light falling on it is scattered and will be reflected in various directions and thus with many different angles. This kind of reflection is known as **diffuse reflection** (Fig. 3.6).

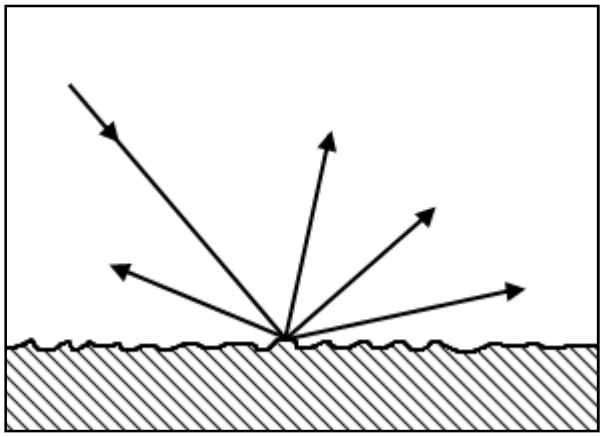

Fig. 3.6 Diffuse reflection

The surface will appear approximately equally bright, no matter the viewing angle. This is known as the **Lambertian reflectance**. This so-called Lambertian surface reflects all light and absorbs none. [6,8,11,12,14,19,36]

The part of light reflected by an object depends on surface properties like its microstructure and the characteristics of the incident illumination such as its spatial and spectral distribution or its polarization. The reflectance can be represented by a function f(i,e,g) of three angles (Fig. 3.7):

- the incident angle θ_i, between the incident light ray and the surface normal
- the emergent angle θ_e, between the emitted light ray and the surface normal
- the phase angle θ_g, between the incident and emitted light light ray

Per definition, the angles θ_i and θ_e are related to a local surface normal.

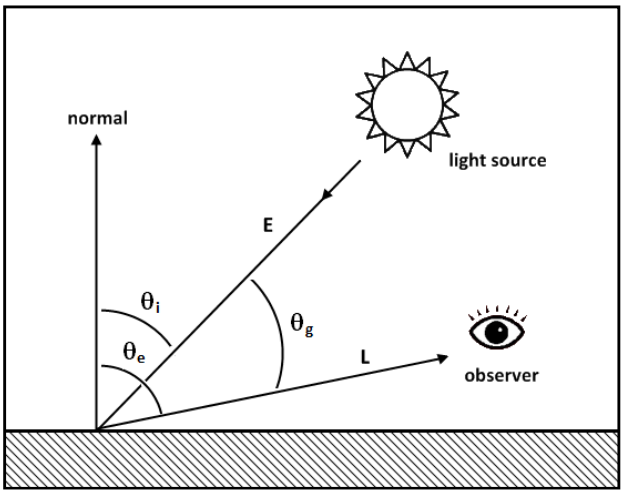

Fig. 3.7 Incident angle i, emergent angle e, phase angle g

The **Lambertian reflectance model** is often used in computer vision to model diffuse reflection and this is also the case for photometric stereo. It is based on Lambert's Law:

$$\frac{1}{\pi} L_i \rho \cos \theta_i \, d\omega \tag{3.1}$$

It expresses a relation between the radiance L_i at the incident angle θ_i and the surface normal through the solid angle $d\omega$. ρ represents the albedo. [*43*]

3.1.3. Radiometric Definitions

Fig. 3.8 illustrates the geometry of the reflectance of a surface patch dA, which is illuminated by a light source from direction $\hat{S} = (\theta_i, \Phi_i)$ and viewed by a person or camera in direction $\hat{V} = (\theta_r, \Phi_r)$

The angle θ corresponds to the polar angles to the z-axis and the angle Φ to the angle measured from the x-axis in the plane perpendicular to the z-axis. E is the incident irradiance, while L corresponds to the reflected radiance.

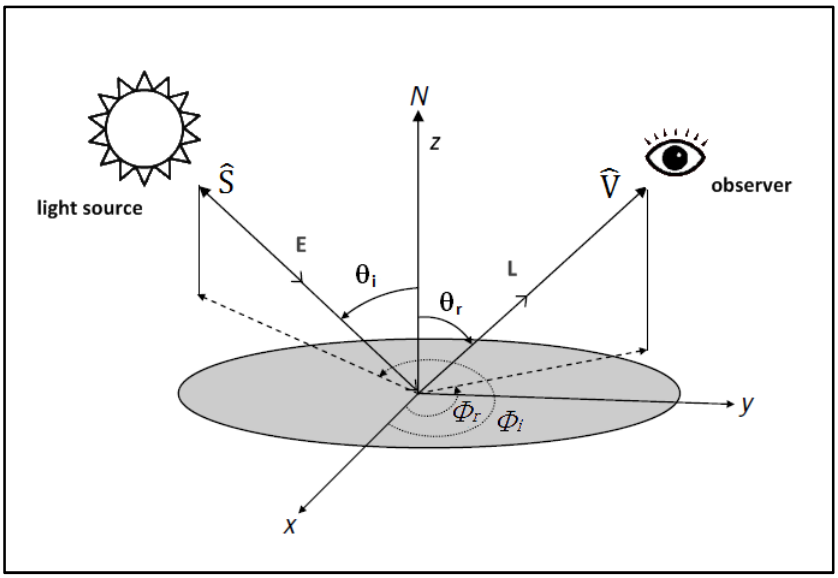

Fig. 3.8 Reflection geometry model (adapted from [*12*])

The incident light energy per unit area of the surface is defined by the **irradiance**:

$$E(\theta_i, \Phi_i) = \frac{d\Phi_i(\theta_i, \Phi_i)}{dA} \tag{3.2}$$

This corresponds to the flux incident in the direction (θ_i, Φ_i), while E represents the flux coming from all directions.

The brightness perceived by the viewer (or camera) is proportional to the surface **radiance**, which corresponds to the light energy emitted per unit solid angle by the surface in direction of the observer:

$$L_r(\theta_r, \Phi_r; \theta_i, \Phi_i) = \frac{d^2\Phi_r(\theta_r, \Phi_r; \theta_i, \Phi_i)}{dA \cdot cos \cdot \theta_r \cdot d\omega_r} \tag{3.3}$$

It is both influenced by the direction of the camera (θ_r, Φ_r) and the direction of the light source (θ_i, Φ_i) . The viewer subtends an infinitesimal solid angle $d\omega_r$. [12,28]

3.1.4. The Bidirectional Reflectance-Distribution Function(BRDF)

The **bidirectional reflectance distribution function (BRDF)** has been defined by the National Bureau of Standards [*27*] as the ratio of the radiance and the irradiance of a surface:

$$f_r(\theta_i, \Phi_i; \theta_r, \Phi_r) = \frac{dL_r(\theta_i, \Phi_i; \theta_r, \Phi_r)}{dE(\theta_i, \Phi_i)} \tag{3.4}$$

In other words, there is a relation between the incident light energy E from the direction of the light source and the reflected brightness L in the direction of the viewer. The BRDF defines how bright a surface illuminated from a direction will appear to a person who is viewing from another direction. [12,17,18,45]

3.1.5. The Orthographic Projection

If the viewing distance is big compared to the size of the object, the radiance of the light source will be a fixed function of these angles, regardless of the surface point which is considered. In order to standardize the image geometry, we choose an orthographic projection as seen in Fig. 3.9:

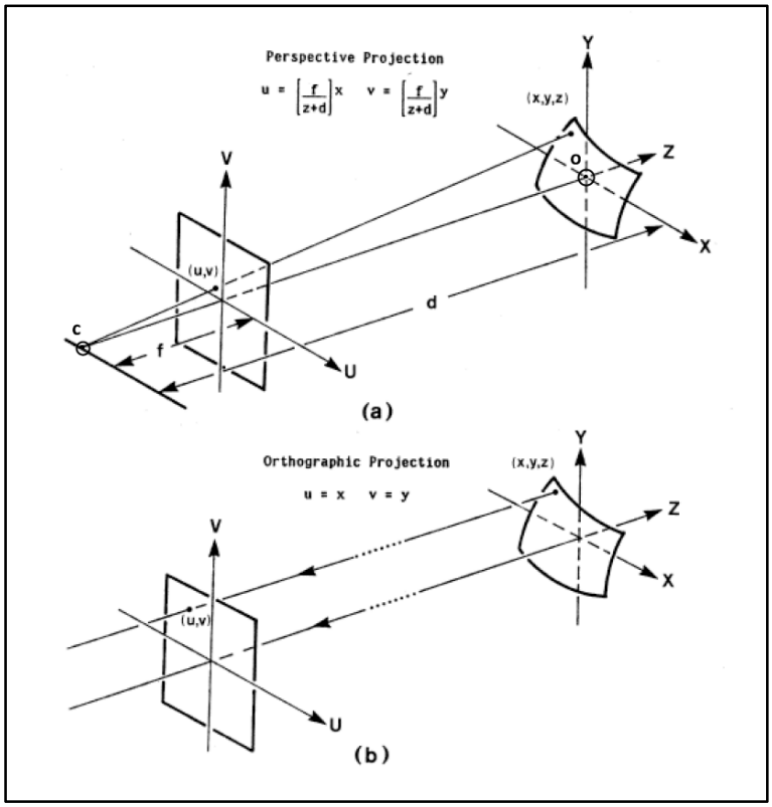

Fig. 3.9 Perspective projection vs. orthographic projection (adapted from [*44*])

In the perspective projection in Fig. 3.9 a), d represents the distance between the origin of the object coordinate o and the center of the lens c while f corresponds to the focal length. In this case, an image point is determined by:

$$(u, v) = (\left[\frac{f}{z+d}\right] x, \left[\frac{f}{z+d}\right] y) \tag{3.5}$$

In the orthographic projection, the focal length f is infinite and therefore all rays from the object to the image are parallel. In this case, we map every object point (x,y,z) to an image point (u,v) where:

$$u = x\,, \qquad v = y \tag{3.6}$$

Thus, we have chosen a coordinate system so that the image plane corresponds to the xy plane and the viewing direction to the negative z-axis. [29,44,45] In this case, the equation of an object surface will be the gradient **space**:

$$z = f(x, y) \tag{3.7}$$

The parameters p and q represent the gradient surface and are defined as:

$$p = \frac{df(x,y)}{dx}, q = \frac{df(x,y)}{dy} \tag{3.8}$$

A surface normal is represented by the vector:

$$[\frac{df(x,y)}{dx}, \frac{df(x,y)}{dy}, -1] \tag{3.9}$$

which turns into:

$$[p, q, -1] \tag{3.10}$$

when we insert (3.8) in (3.9). [13,29,38,45]

3.1.6. The Reflectance Map

In section 3.1.4, we have seen that the brightness of a surface depends on the orientation of the surface to the observer and the light source. If the surface is not planar, the reflected light will not be the same for every part, depending on the position in space, as shown in Fig. 3.10:

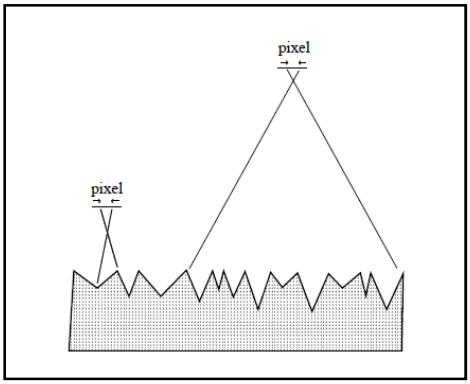

Fig. 3.10 Influence of the roughness on the reflectance properties of a surface [*28*]

Therefore, the image will show some shadows, which in turn provide some information about the shape of the object. This information can be captured by a reflectance map described below. The latter represents the image radiance as a function of **surface gradient** in an orthographic projection. In this case, the incident angle θ_i and the emergent angle θ_e depend only on surface orientation, the phase angle θ_g and the direction to the observer are constant. As a result, the image intensity can be determined with a function of p and q, the **reflectance map** R[17,23,29,44,45]:

$$R(p,q) \tag{3.11}$$

In other words, the reflectance map gives some information about the surface reflectance for a certain geometry of a light source and a viewer. It shows the dependence of scene radiance on surface orientation.

3.1.7. Three Channel Dynamic Photometric Stereo

Using the reflectance map, the basic equation describing the image-forming process can be written as:

$$I(x,y) = R(p,q) \tag{3.12}$$

According to Woodham [*44*], the incident illumination patch has to be constant at every surface and the projection has to be orthographic in order to fulfill (3.12).

This equation can be used in image analysis to determine object shape from image intensity, which is fundamental in the process of shape from shading and photometric stereo, respectively. Photometric stereo is a reflectance map technique that uses two or more images to solve this equation directly. [29,45]

Suppose three different incident illuminations of the same object with the corresponding images $I_1(x,y)$, $I_2(x,y)$, $I_3(x,y)$. According to the basic image-forming equation (3.12), we will get the following three reflectance maps R_1, R_2, R_3:

$$I_1(x,y) = R_1(p,q) \tag{3.13}$$
$$I_2(x,y) = R_2(p,q) \tag{3.14}$$
$$I_3(x,y) = R_3(p,q) \tag{3.15}$$

The intensity values of a point (x,y) can be represented as the vector $\vec{I}$:

$$\vec{I} = \begin{bmatrix} I_1(x,y) \\ I_2(x,y) \\ I_3(x,y) \end{bmatrix} \tag{3.16}$$

The three lighting direction vectors $\overrightarrow{s_1}$, $\overrightarrow{s_2}$, $\overrightarrow{s_3}$ are defined by:

$$\overrightarrow{s_1} = \begin{bmatrix} s_{11} \\ s_{12} \\ s_{13} \end{bmatrix}, \qquad \overrightarrow{s_2} = \begin{bmatrix} s_{21} \\ s_{22} \\ s_{23} \end{bmatrix}, \qquad \overrightarrow{s_3} = \begin{bmatrix} s_{31} \\ s_{32} \\ s_{33} \end{bmatrix} \tag{3.17}$$

Stacking these vectors row by row gives the following illumination matrix ***S***:

$$[\boldsymbol{S}] = \begin{bmatrix} s_{11} & s_{12} & s_{13} \\ s_{21} & s_{22} & s_{23} \\ s_{31} & s_{32} & s_{33} \end{bmatrix} \tag{3.18}$$

If we take a surface element with the albedo ρ and the normal $\vec{N}$ from the illuminated object, the intensity can be characterized by:

$$\vec{I} = \rho[\boldsymbol{S}]\vec{N} \tag{3.19}$$

If the three light directions are not in the same plane, the inverse of $[\boldsymbol{S}]$ exists, so that:

$$\rho\vec{N} = [\boldsymbol{S}]^{-1}\vec{I} \tag{3.20}$$

Repeating this procedure for every surface point will lead to the gradient field *G*:

$$G = (p(x,y), q(x,y)) \tag{3.21}$$

3.1.8. Depth Recovery From Gradient Field

In order to get a surface depth function $Z(x,y)$, the gradient field from equation (3.21) has to be integrated. There is a big variety of integration methods which can be separated in local and global techniques.

When integrating locally [5,46], an initial height value Z_0 is preset for a starting point (x_0, y_0) in the surface. The relative depth value at every point (x,y) will then be calculated, according to a local approximation rule. The advantage of local integration is that the techniques are simple and fast. As they depend on data accuracy, they will therefore propagate any measurement error along the process.

Global integration methods [9,20,21,22,31,34,35,42,47] on the other hand will calculate the depth function $Z(x,y)$ by minimizing the quadratic error functional *W* between ideal and given gradient values:

$$W = \iint \left[|Z_x - p|^2 + |Z_y - q|^2\right] dxdy \tag{3.22}$$

Integrating globally brings the advantage that there is no error propagation as errors will be evenly distributed over all points. On the other hand, these methods require a complex implementation.

The predominating methods for global integration are: the **four-scan-method** used by Klette and Schlüns [*22*] as well as Horn [*20*], the **method of Frankot and Chellapa** [*9*], the **Gauss-Seidel technique** [*21*], the **Successive Overrelaxation (SOR)** [31,35] and methods based on **Fourier transformation** [42,47]. In this work, the integration of the gradient field has been done with the method of Frankot and Chellapa [*9*].

3.2. Local andTechnical Prerequisites

Some local and technical conditions had to be taken in consideration before setting up the video capturing system. The setup of the video capturing system used for this work is based on the research of Schulze [*35*] which gives some further information about the physics of the system, its possibilities and restrictions when applyied it in practice, and the work of Schroeder [*33*] which made an extended fundamental mathematical research for this system.

3.2.1. Local Situation

The presented work has been carried out at the rehabilitation department of the Wan Fang Hospital in Taipei, Taiwan. The hospital with 758 beds and 320 employees is publicly owned, but privately operated and has been accredited with the International Quality Certificate of ISO-9002 in 2006. [*39*]

Two rooms have been provided for this research. One of them was an office which was shared with other employees of the rehabilitation department and which was accessible around the clock. This room has been used for the paperwork, the video evaluation, the programming work and every other computational task. The video capture on the other hand took place in a therapeutic exercise room of the rehabilitation department. This place was used for patient treatment and exercises by the physical therapists of the department. In avoidance of disturbing the daily routine, the room could be accessed only at night and Sundays. Therefore, the video capturing system had to be installed and deinstalled for every record. For practical reasons and for making the system calibration more accurate, the light sources had been fixed on the ceiling [*35*], so that only the cameras and the calibration material had to be mounted.

3.2.2. Technical Material

The following technical material has been employed for this work:

- ***Light sources with dichroic color filters***

The room was illuminated by six dimmable light heads of the type Dedolight DLHM4-300E with an integrated 24V/150W electric power supply [*7*] and a movable head for adjusting the operating position the lighting direction, respectively. The dimmer was turned on to the maximum for every lamp in order to get the maximum of light available while recording.

For creating red, green and blue light sources, every lamp was equipped with a dichroic filter in the appropriate color. The principle of dichroic filters will shortly be explained. To understand the difference to a conventional color filter, consider a filter which is expected to “create” the color Magenta as shown in Fig. 3.11:

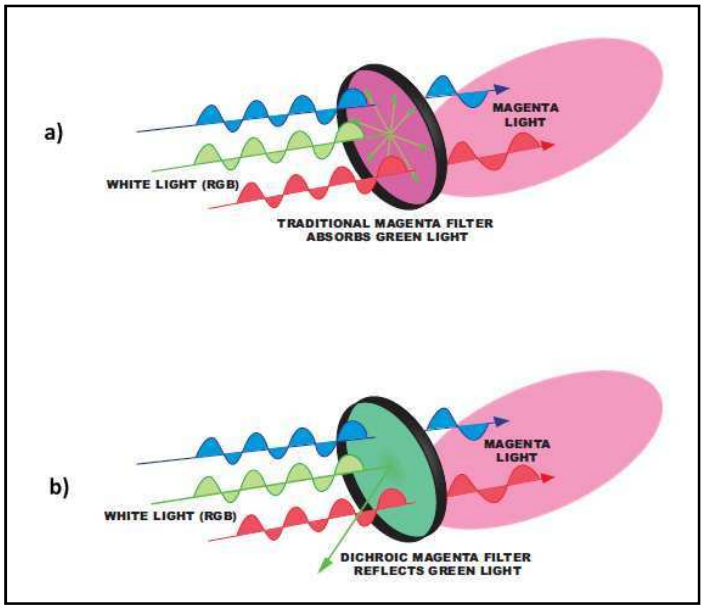

Fig. 3.11 Magenta filter: conventional filter vs. dichroic filter [*32*]

A traditional color filter absorbs certain wavelengths of light (in this case green light) and transmits the part of the light corresponding to the filter color (Magenta), so both the filter and the transmitted light appears in the same color Magenta (Fig. 3.11 a)). A dichroic color filter however reflects these wavelengths (green light) and transmits the rest of the spectrum (Magenta). Consequently, the filter is perceived in green while the transmitted light is still Magenta (Fig. 3.11 b)).

Besides creating highly saturated colors, dichroic filters have a longer durability as their thermal stability is higher than for a conventional color filter.

The lights themselves were arranged in two groups of three lamps (red, green, blue) on both sides of the room (Fig. 3.12).

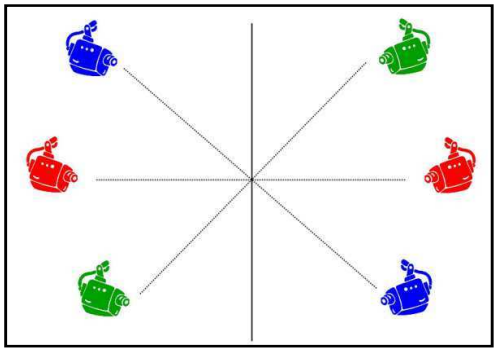

Fig. 3.12 Lighting setup

- ***Cameras***

Three Sony HDR-HC5 Video Camera Recorders were used to make the recordings from the front, the back and the side of the subject. One supplement camera was provided as a spare camera in case of technical problems. The videos were taken in HD resolution of 1440x780 pixels and stored on mini digital video tapes. The cameras themselves were labeled with numbers from 1 to 3 corresponding to the front, back and side camera and used at this place for every video capture.

- ***Tripods***

For recording, the cameras were fixed on tripods of the type *Manfrotto 718B DIGI MINI 3W Tripod BLK*, a compact 4-section tripod with a built-in hybrid video/photo 3-way head with a "dovetail" quick release camera plate, separate pan and tilt locks and short pan/tilt bar. [*24*] The plate allowed the camera to be quickly mounted on and unmounted from the tripod.

Besides the three tripods utilized for fixing the cameras, a fourth was needed for holding the calibration balls in place (see section 3.3.2).

- ***Flash light***

An external flash unit was used for the synchronization of the three video records (a detailed description can be found in section 3.3.3) in order to get a three-dimensional reconstruction at the process end.

- ***Computers***

A personal computer with a FireWire interface was used for the import of the video recording, the data processing, evaluation and saving and also for programming tasks. The Linux distribution FedoraCore 13 was running on the PC. For practical reasons, a notebook was also used for the same tasks, which had Windows 7 as operating system. A remote access was configured from the notebook to the personal computer, so that the important data which was stored on the stationary computer was available all the time.

3.2.3. Software and Programming

The program ***Dynamic Photometric Stereo (DynPS)*** which has been developed by Schroeder and Schulze [34,35] was the basis of this work. It is described in section 3.3.4. The program is written in ***Interactive Data Language (IDL)***. This scripting language is often used for data analysis, visualization and cross-platform application development as it provides a lot of operators and functions for the presentation of data, volumes and images. The IDL widgets are a useful tool for programming platform independent graphical user interfaces, which was a part of this work, too.
Besides the main part programmed in IDL, a few parts are written in ***C++***, in order to reduce the compilation time.

For accomplishing the tasks of this work, some additional software has been used. The software development for the graphical user interface has been done with the program ***Emacs***, an open-Source text editor which provides syntax highlighting of the program code.

As the DynPS application was intended to be used on a Linux system and the notebook was running on Windows, the software ***Cygwin*** was installed on the portable computer, making it possible to port the software running on Linux to Windows. The remote access software ***RealVNC Viewer*** on the notebook enabled to interact with desktop applications on the personal computer.

3.3. Working Procedure

As the intention was to have similar working conditions for every video capture to have comparable 3D reconstructions at the end of the process, it was necessary to regulate the working steps and to make them reproducible. The following sections give essential information about the way this task has been solved.

3.3.1. System Setup

Schulze described the setup of the system in detail in his work [*35*]. The setting has been adopted and is shown in Fig. 3.13. As already told before, a set of a red, a green and a blue light source has been fixed at every long side of the room. Three cameras had to be installed: no. 1 for the front, no. 2 for the back and no. 3 for the side view. Each of them was attached on a tripod with the legs extended to the maximum. The positions of the tripods and the subject plane were marked on the floor, and the material itself was marked with numbers 1-3 for every pair of camera and tripod. These precautions assured the constancy of the filming conditions over every recording sequence.

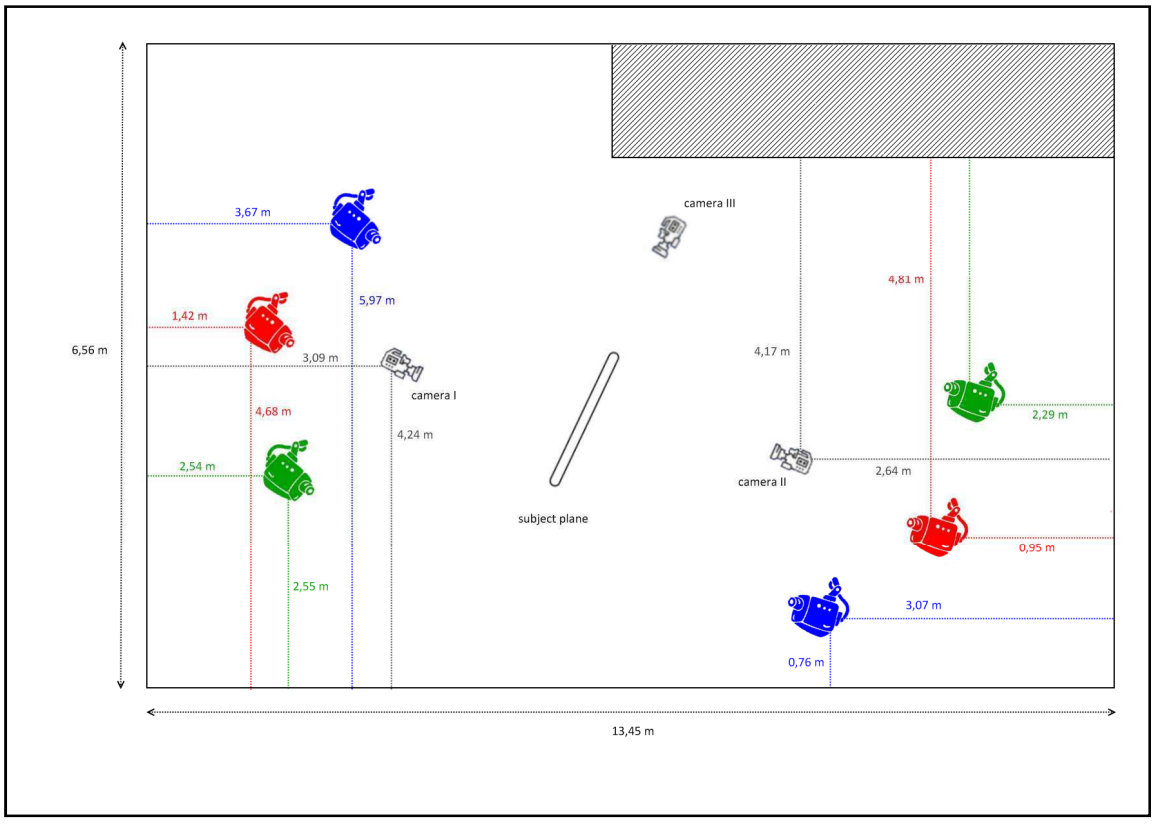

Fig. 3.13 Schematic representation of the video system setup in the therapeutic exercise room (based on [*35*])

As there was a period of two years between Schulze's work and this one, some adjustment had to be undertaken. The direction of the light sources fixed at the ceiling had to be corrected so that for both sides the three lights pointed to the same spot. The marks on the floor where to place the cameras 1 and 2 had been rubbed out, so that their right positions had to be found and marked again. Finally, the distances between the cameras and the walls of the room were almost as described by Schulze, with a few irrelevant differences of less than 1 cm. The plane where the filmed subject (calibration board, dummy, patient) had to stand also had to be found and marked. After these corrections, the

reproducibility of the system setup was guaranteed for every recording and after every installation and deinstallation, respectively.

The guideline for the system setup *Manual for Dynamic Photometric Stereo Application* originally written by Schulze [*35*] has been completed an adapted during this work, which describes the setup process step by step.

3.3.2. Calibration and Empty Frame

As the intention of this work was to improve the quality of the 3D reconstruction with photometric stereo, it was essential to generate video recordings with the constant quality in order to assure the comparability. For this purpose, the system had to be calibrated. This was realized by using a whiteboard which was placed in the middle of and orthogonally to the front camera 1 and the back camera 2. In addition, it had to be taken into account that the side camera 3 had an adequate filming frame and was capturing the whole subject. The whiteboard itself was fixed on rolls to be easily movable. In order to ensure the Lambertian reflectance model, the board's surface was smooth and untextured. One crucial point of the calibration was that the light three light sources met each other on both sides of the whiteboard, so that its color appeared white. If this wasn't given, the directions of the lamps had to be corrected.
The calibration was based on the method of Schroeder et al. [33,34], who proposed a light source calibration with a metallic sphere with specular reflection properties. The calibration ball was intended to be put on the fourth tripod during the calibration (see Fig. 3.14), thus its weight was limited.

Fig. 3.14 Example of a calibration sphere illuminated by the three light sources

As it was impossible to find a light sphere with metallic character, a rubber ball with a shiny surface was employed instead. Since one task of this work was to improve the calibration of the system (see section 3.4.1), different calibration balls were bought and tried out in order to find out which one yielded the best calibration results, but all with the properties described above.

The distance between the camera and the whiteboard had to be measured with a laser range finder for all three cameras, as well as between the camera and the calibration sphere for cameras no. 1 and no. 2. Besides that, a few frames of the empty room without the whiteboard but with the same light conditions were needed, called “empty frame” in the application DynPS.

3.3.3. Synchronisation and Recording

After the calibration and the capture of the empty frame, the subject intended to be filmed could be placed on the same position as the white panel previously. The distance between the camera no. 1 (respectively no. 2) and the subject was measured with the laser range finder.

A crucial point for getting a good 3D reconstruction of the subject was to get synchronized sequences of the three videos from the different cameras. This could be done by firing a single flash with a flash unit, which appeared to be the best method for synchronization in Schulze’s work [*35*]. The shooting of the flash was recognized by the program as the synchronization point and therefore the starting point of the same video sequence for the three cameras.

Recording was started with all three cameras. At this point, the flash unit was used for firing the initial synchronization point. The dummy or the person was filmed for a few minutes with or without moving. As the rotation around the longitudinal axis is not supported for the moment [*35*], the patient was asked to move in the transversal plane, bending down right and left with the arms extended or just moving the arms up and down.

Once the video sequences were taken, the video capturing system was deinstalled and the following work was done on the computer with the program *DynPS*.

3.3.4. Program Steps

This section will give a short description of the functions of the program *Dynamic Photometric Stereo (DynPS)*, which is used to transfer the video recordings on the computer and to process them in several steps into the 3D reconstruction. A more detailed explication of these different stages in the reconstruction process with the help of DynPS will be the subject of the section 4.2. For now, Fig. 3.15 will give an overview of the whole 3D reconstruction process split into the single steps.

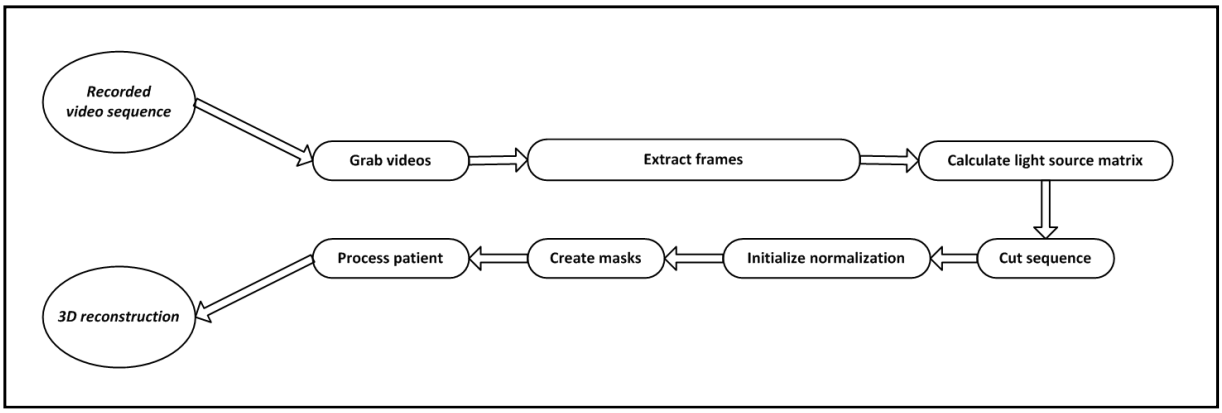

Fig. 3.15 Overview of the 3D reconstruction process steps

The first step in the whole process is to upload the recorded video sequences on the computer. For this, the camera is connected with a FireWire cable to the PC and the menu point ***"grab videos"*** is chosen. During the ***frame extraction***, the video is then split in several single frames which are saved on the computer. By clicking on ***"Calculate light source matrix"***, the light source calibration begins. For this, the frames of the calibration sphere are needed. The ball has been placed in the scene so that its center matches to the center of the camera's coordinate system. With the diameter of the calibration ball (which is calculated with the points the user assigns to be the top, the bottom, the rightest and the leftest on the calibration sphere), the location of the light source related to the camera can be calculated. . [*35*]

An essential part of the recording was to fire the flash unit in order to synchronize the three videos. When ***cutting the sequence***, the program is going through all the extracted frames in order to find a significant change in the image brightness. As the illumination is constant during the whole video capture, this massive lighting change represents the point where the flash was fired. At these points, the video sequence is cut so that for all of the three cameras, the first frame in the series happened at exactly the same point of time when taking the video.

For Dynamic Photometric Stereo, the assumption is made that the light illuminating the scene comes from a point light source. In reality, this can only be achieved when distances between the light sources and the image scene are big. As this was not possible in the therapeutic exercise room, a ***light source normalization*** using the reference frame took place as a correcting mechanism.

In order to reduce the amount of data and size processed, a mask of the input frame is created. The algorithm of the ***mask creation*** as well as the succeeding patient processing have been explained extensively in Schulze's work [*35*] and would not be taken up at this place.

3.4. Planned Experiments

The aim of this work was to continue the research of Schroeder and Schulze [33,34,35] and to improve their presented method of Dynamic Photometric Stereo in order to make the quality of 3D reconstruction at the end of the process better and to have a program which works with "real patients". This chapter will explain on which points the method could be improved.

3.4.1. Improvement of the Light Calibration

A better quality of the 3D reconstruction can be reached when the system is getting more accurate. One possibility is to improve the light calibration as it will have an impact on the basis of the process and therefore make the results more precise. The ideal calibration ball is supposed to be a metallic, shiny sphere with Lambertian properties (see section 3.3.2). Also, its diameter plays a role in the evaluation of the results. So the challenging task was to find balls which fulfill these conditions best. When using different balls, the results at the end of the process will also be different. Thus, the idea was to compare the results of the 3D reconstructions based on different calibrations in order to find out the best calibration sphere.

At the end, a set of five balls of different colors, materials and sizes were tried out (Fig. 3.16):

- Shiny blue rubber ball (a)
- Matte blue rubber ball (b)
- Shiny cream rubber ball (c)
- Multicolored beachball (d)
- Huge blue beachball (e)

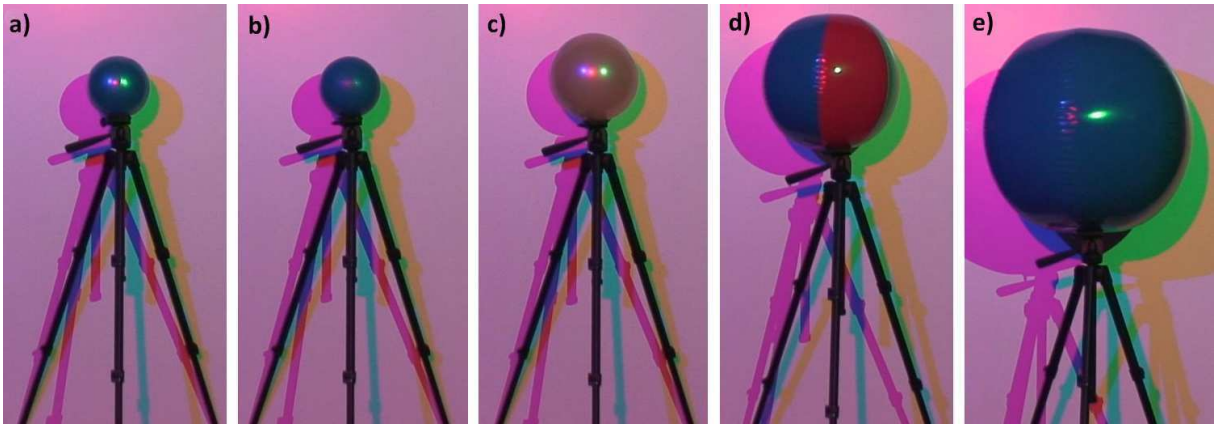

Fig. 3.16 The different calibration balls

3.4.2. Improvement of the 3D Image Reconstruction

Another way of getting more accurate results is to change the aspect of the filmed patient. The different ways of achieving this are shown in this section.

3.4.2.1. White Shirt

The surface of the human skin is not even, but shows some irregularities in the color and the texture like pigmentations, belly buttons, nipples, etc. At these points the light will be reflected differently. Distortions will appear which is finally resulting in unsharp 3D reconstructions.

To avoid these phenomena, some methods should be found to make the skin surface more even and more unicolored. The first idea was to use a thin and tight white shirt. The challenge was to find a white shirt with the following properties:

- white or cream color
- the shirt tissue should not be too transparent
- large enough to fit a person of average height and weight, but tight enough so that it doesn't make any wrinkles
- long sleeves without seams at the wrist
- a collar without neckline, where the neck skin doesn't look out from under the collar

As these characteristics could not be fulfilled entirely, a compromise had to be found. Two shirts were used finally, a very tight shirt with short sleeves and a long sleeve shirt with seams at the wrist.

Fig. 3.17 White shirts with short sleeves (A) and with long sleeves and wrist seams (B)

Wearing a tight white garment could also be considered for the legs if some adequate pants are found. During this work, this task was not possible as it was summer and it was too difficult to find some tights.

3.4.2.2. Abdominal Circumference and Shift of the Center Mass

Schulze already showed a correlation between the circumference and the volume of a patient when measuring pregnant women at two different time points [*35*]. The goal was to continue this work and to make some measurements for other pregnant subjects.

Moreover, Schulze calculated and visualized the shift of the center of mass for each volume, assuming an even distribution of the body mass. The intention was to conduct research on this field as well. For this, a machine used by the occupational therapists for measuring body balance parameters was available and could be integrated into the program.

3.4.3. Improvement of the User Interface

Previously, the functionality of the application was prioritized. Therefore, the graphical user interface was implemented in order to make it simple to use for the researchers themselves. The main goal of this work, however, was to make the whole method smoother, so that it can be used by non technically-orientated staff. As a lot of value inputs happened on the IDL console, which is not convenient for persons without background in informatics, the program needed some improvements at the graphical user interface.

The different program steps were first analyzed one after the other and the critical points were detected. The main changes were made at the different value inputs. Every single IDL console input has been redirected on a convenient and self-explaining input frame. The user can now easily enter the values, without having to switch between the IDL console and the DynPS application. Besides that, explications were added for the choice of different files and directories. Also, new selection frames were implemented so that the user has the possibility to find more quickly the directories and are able to cancel almost every step. Finally, a flexible threshold value has been introduced for the front- and the back camera for the masking process.

The different elements of the graphical user interface and the user interaction will be explained in section 4.2.1.

4. Results

The intention was to describe the results in the same order as the experiments presented in section 3.4. Unfortunately, several problems appeared during this work, so that this can't be done for every experiment. Instead of that, the encountered problems will be elucidated.

4.1. Encountered Problems

4.1.1. Technical Problems

The whole work was disturbed by a lot of technical problems which will be described in this section. At the beginning, the future development of the different problems and the consequences for the work were not known. The following explications will therefore attempt to reconstruct chronologically the difficulties as completely as possible.

The first task in the work was to run the application DynPS on the personal notebook. As the application is running on Linux, but Windows 7 was installed on the computer, some configurations had to be done to run the program. After the successful installation of the provided code files, the program should have been able to start. But already at this point, the first problem occurred. Although the application was running in the work done before [34,35], it wasn't for most of the program steps at this time. A long debugging process was started in order to find out the causes. Every process in the application was debugged one after the other as they are based on each other. Apart from the "grabbing" process, none of the steps was running properly at the beginning and all caused different kinds of error messages. Unfortunately, the different debugging processes haven't been documented, as the extent of the code problems was not known at this point of the research and the intention of this work was not to explain errors.

The main part of the problems was about the code used in the application itself. But also the material broke down at a point where some videos should have been taken. One of the light bulbs did not work which delayed the project even more as the order of this special material took two weeks.

Just after the bulb had been inserted into the light, one of the cameras wasn't working anymore. The tape head was dirty and a cleaning cassette had to be bought. The newly purchased tape was not working and had to be exchanged. This problem therefore also took more than one week until the camera was working again. Note that at this time, only 3 cameras were available and no video capture was therefore possible.

At the end of the stay in Taiwan and after long months of debugging and problem solving, the most important problem was discovered. It was noticed that the code which had been provided at the very beginning of the stay was not the newest one, but an older version of the code. This discovery explained why the aforementioned processes didn't work at the early beginning of the stay in Taiwan. The time remaining was at this point not enough to complete the intended work.

4.1.2. Human Communication

When different humans are working on the same project with a common goal, the most important task at the very beginning is to define the expectations of every participant. Good communication is the key for the success of a project (Fig. 4.1).

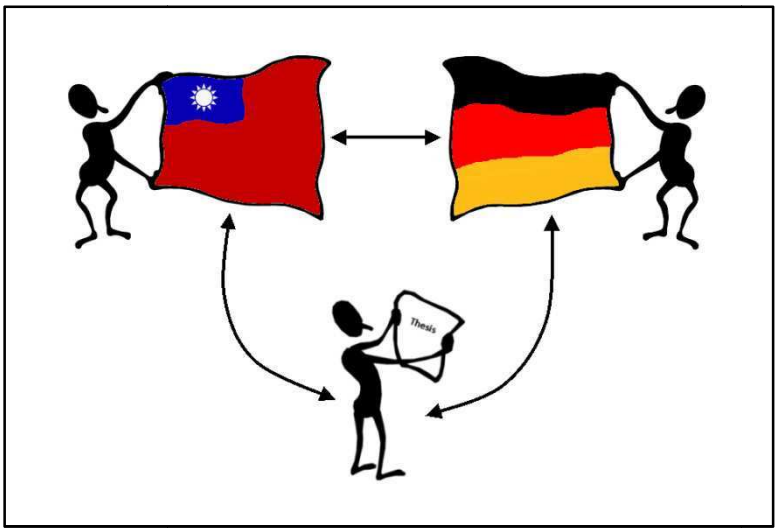

Fig. 4.1 Communication between the Taiwanese advisor, the German advisor and the student

During this work, the expectations for every side were not discussed enough and the communication was occasionally unilateral as the focus was not the same for everyone. A lot of assumptions have been made on every side, so that it resulted in a failure of the whole project. For a next candidate who wishes to continue on this work, the expectations and the tasks for every person should be defined clearly. This was not the case during this work, so that they couldn't be fulfilled properly by everyone.

Also, the preparation should have been done more meticulously on both sides. If the program had been tested once before the project started, a lot of false conclusions could have been avoided and at the end a better result could have been reached.

4.2. Working Steps

One of the goals of this thesis was to document the current state in the research made by Schroeder and Schulze [33,34,35] and this text itself in order to build a good starting position for potential further researchers on this topic.
This section will go through the single program steps of the application Dynamic Photometric Stereo (DynPS) and will elucidate what the program does at every stage. Some theoretical knowledge will also be given when it is necessary to understand the process.

Fig. 4.2 shows the user interface when the DynPS application has been started and gives an overview of the different application functions.

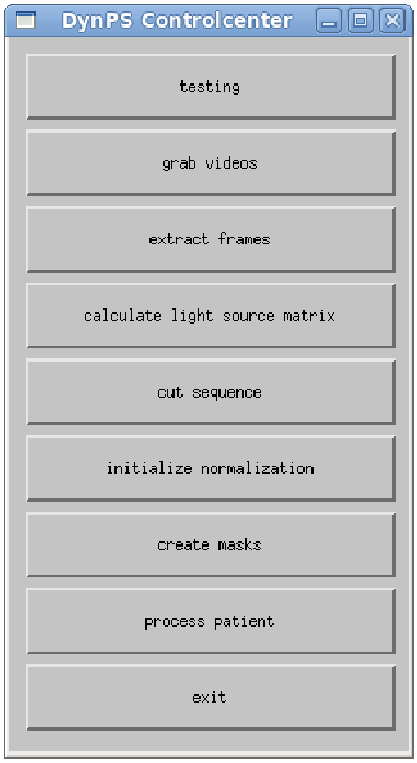

Fig. 4.2 Starting panel of the DynPS program

4.2.1. Program Steps

So far, the interaction between the program and the user was happening partly on the desktop with the graphical user interface, but more often on the IDL console. The latter is a simple and fast tool for a person with good informatics knowledge, but it is not appropriate for user from other backgrounds. Also, it is not convenient for hospital staff in their daily life to have to change from the console to the graphical user interface and vice versa for every single step in the program. Their working processes have to stay as smooth as possible in order to guarantee good healthcare.

These are the reasons why the graphical user interface has been improved during this work. The upgradings are described in this section for every single step in the DynPS application. For each of them, an activity diagram has been created for demonstrating the interaction between the user and the system and a better overview of the program.

4.2.1.1. Video Grabbing

Firstly, the recorded video sequences have to be uploaded on the computer. For this, the user has to start the program and click the option “grab” on the starting panel. The activity diagram in Fig. 4.3 illustrates the succession of the initiated events.

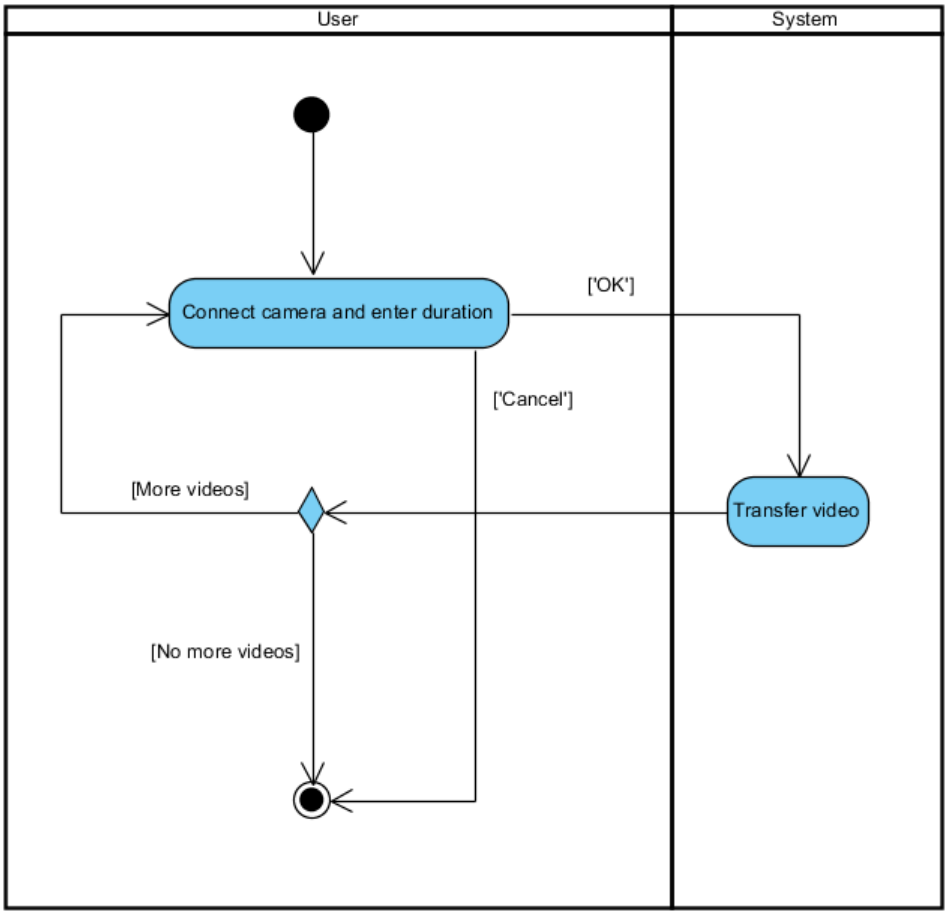

Fig. 4.3 Activity diagram of the process “grabbing”

The program asks to connect the camera to the computer, to rewind the tape and to switch the camera into playback mode. Besides that, the recording time of the uploading video has to be entered as shown in Fig. 4.4:

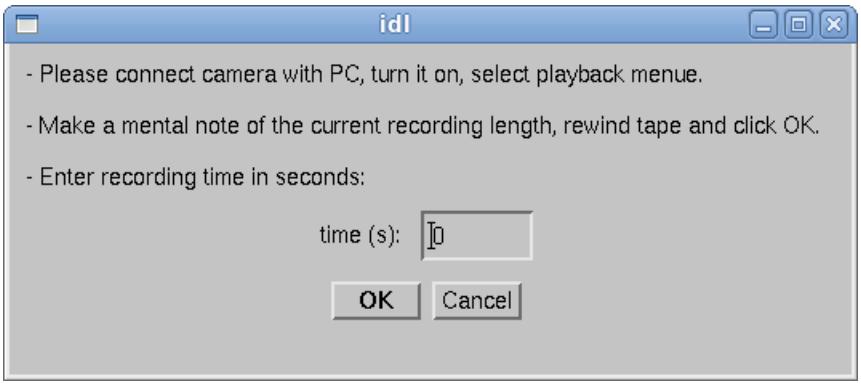

Fig. 4.4 Input panel for grabbing a video

The program then renames the video b in the form "*#.m2t",* where # represents the number of the video uploaded for every grabbing action, before it is stored in the directory "*/videos/<Date>*" created by the application.

This process is repeated as long as the user approves to upload more videos (Fig. 4.5) and is finished if he denies it.

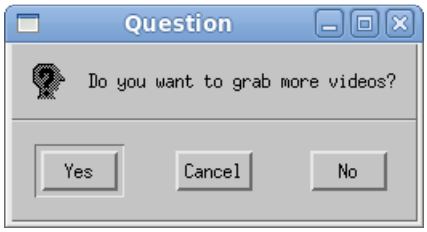

Fig. 4.5 Pop-up for uploading more videos

In this case, the user is informed of the successful ending of the procedure (Fig. 4.6).

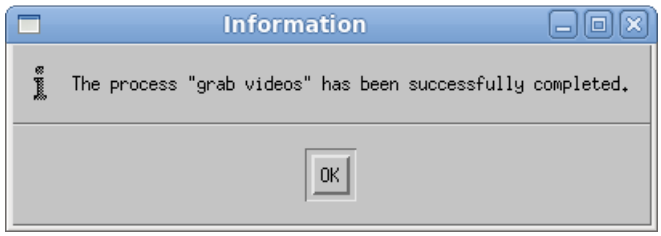

Fig. 4.6 Confirmation of completed process "grab videos"

4.2.1.2. Frame Extraction

As shown in the activity diagram of Fig. 4.8, the main task for the user during the "frame extraction" is to indicate the directories of the video sequence to be partitioned in single frames and of the place where the extracted frames have to be saved (Fig. 4.7)

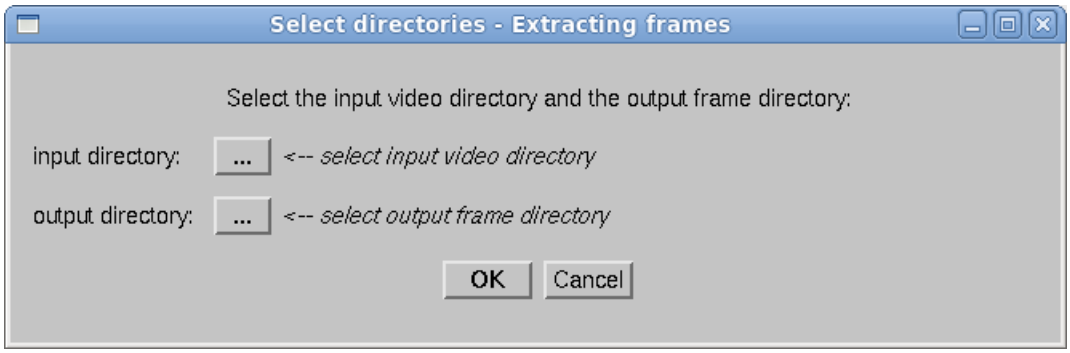

Fig. 4.7 Selection panel for input and output directories

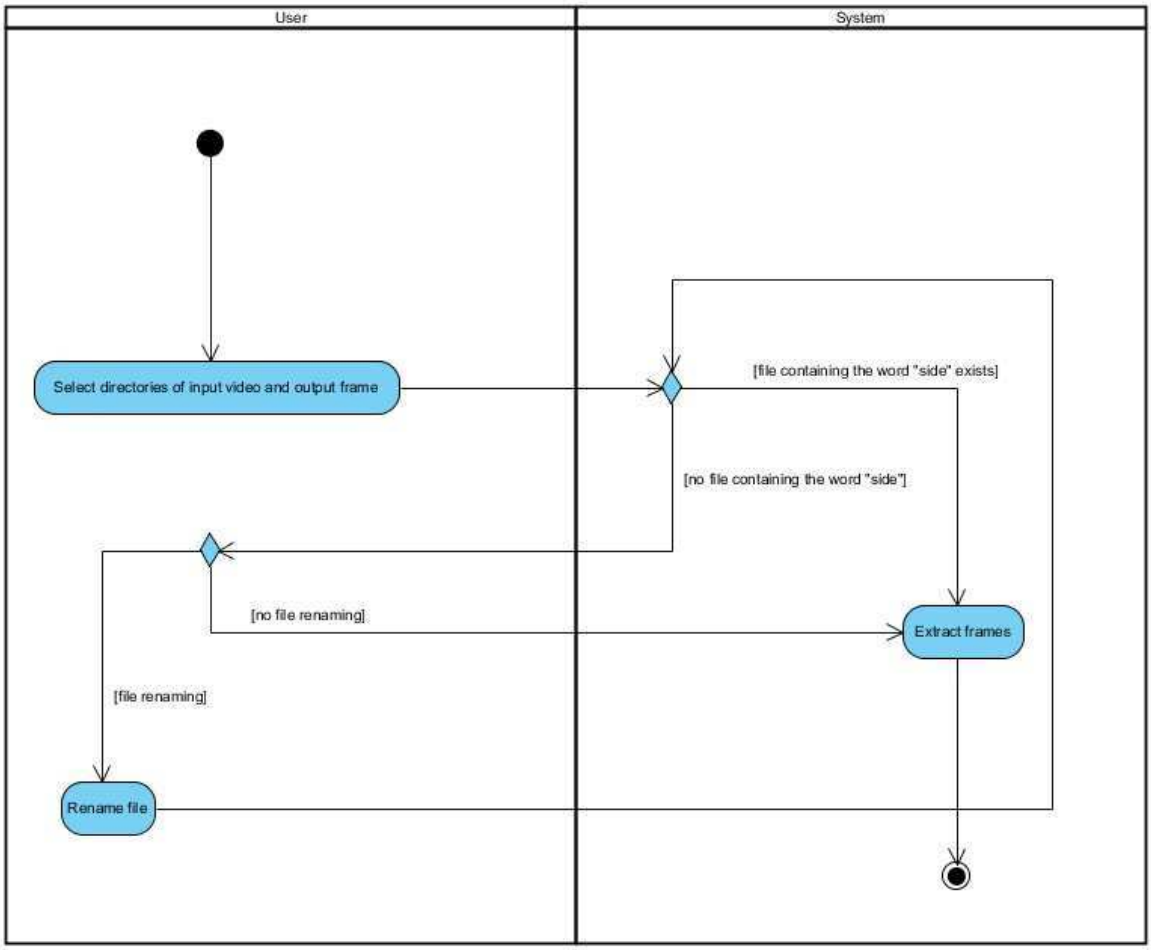

Fig. 4.8 Activity diagram of the process "frame extraction"

The application then goes through this input directory and checks the presence of a file containing the word “side”. This is an important aspect as the videos taken from the side are rotated and the code is implemented so that they are recognized by including the name “side”. If no such file exists in the directory, the user can choose to rename a file or to continue the extraction (Fig. 4.9):

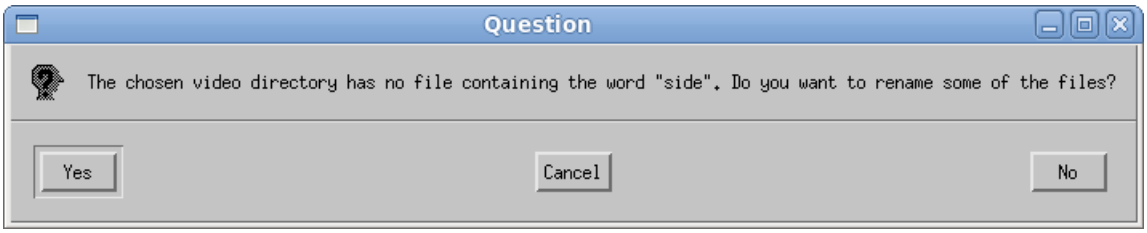

Fig. 4.9 Question to rename a file

In the case he affirms this question, the user is solicited to indicate the file which he wants to rename and the new name to be assigned to the file (Fig. 4.10).

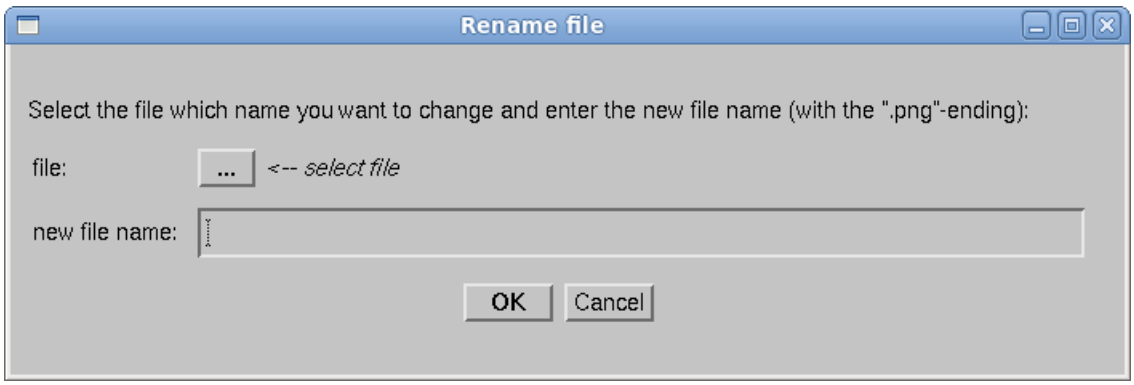

Fig. 4.10 Panel for renaming a file

If the directory contains a file including the word “side” or the user doesn’t want to rename a file, the frame extraction begins. The open source media player mplayer and the video processing tool mencoder are used for this task. At the end of the process, the user is informed about the successful ending of the frame extraction.

4.2.1.3. Light Source Matrix

The process of the light calibration is done when the user clicks on “calculate light source matrix” (Fig. 4.11). The program will create the matrix for the light source calibration which is needed for the following processing steps.

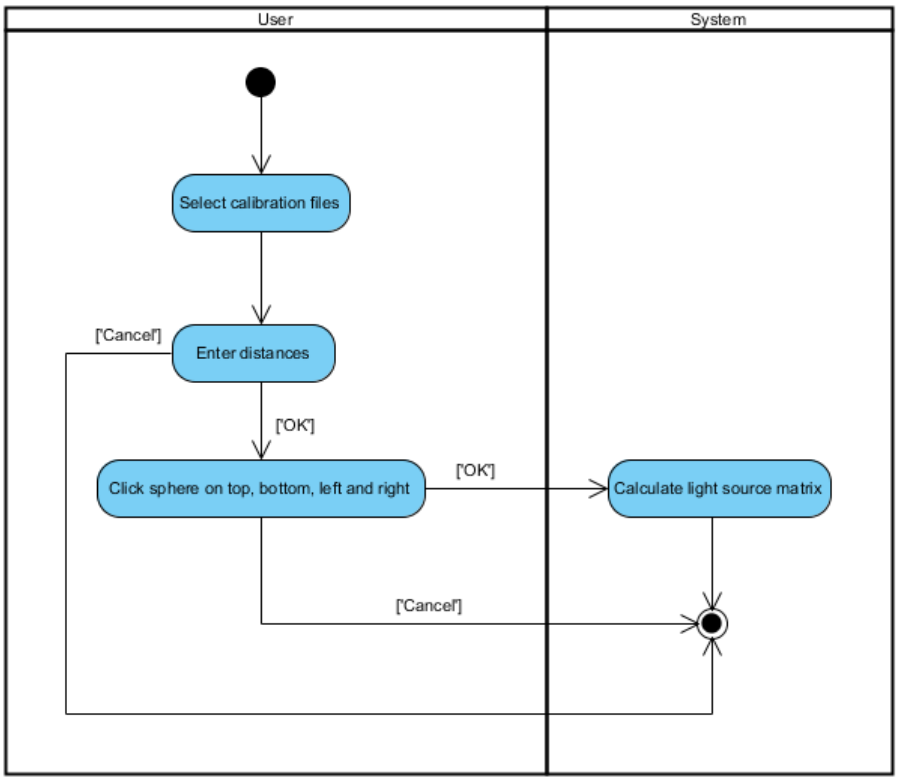

Fig. 4.11 Activity diagram for the process "Light source matrix"

The user is prompted to indicate the calibration files for the camera no.1 and no.2 (Fig. 4.12). Also, he has to enter the distances between the whiteboard and the cameras no.1-3 as well as between the ball and the cameras no.1 and no.2 (Fig. 4.13).

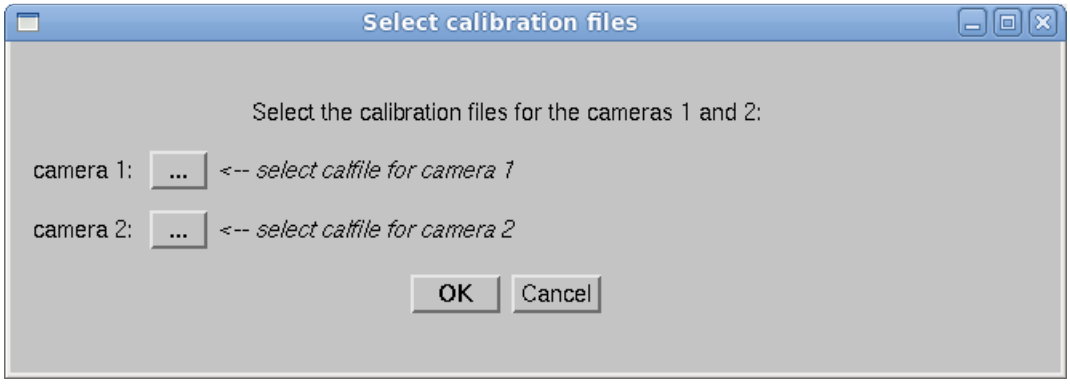

Fig. 4.12 Selection panel for calibration files for cameras 1 and 2

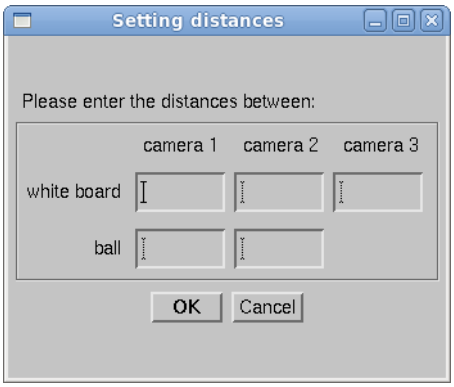

Fig. 4.13 Input panel for distances

After confirming the entered values, the process of extraction itself begins. The user has to click on the top, the bottom, the left and the right boundary of the sphere, which is combined in one action field on the activity diagram in Fig. 4.11. Based on this, the program can calculate the diameter of the calibration sphere and with the help of the distance between the camera and the ball, the matrix for the sphere. This matrix is then corrected in order to match its coordinates to the one of the camera. The resulting matrix is saved for the later use in subsequent events. The whole process is performed twice for both front and back viewing cameras no. 1 and 2.

4.2.1.4. Cutting Sequence

Cutting the frames into sequences regarding the brightness of the scene is the main task of the fourth step (Fig. 4.14). First, the user has to select the directories of the frames which he wants to break down into several parts for all three cameras (Fig. 4.15) and the directories of the empty frames for camera no. 1 and 2 (Fig. 4.16).

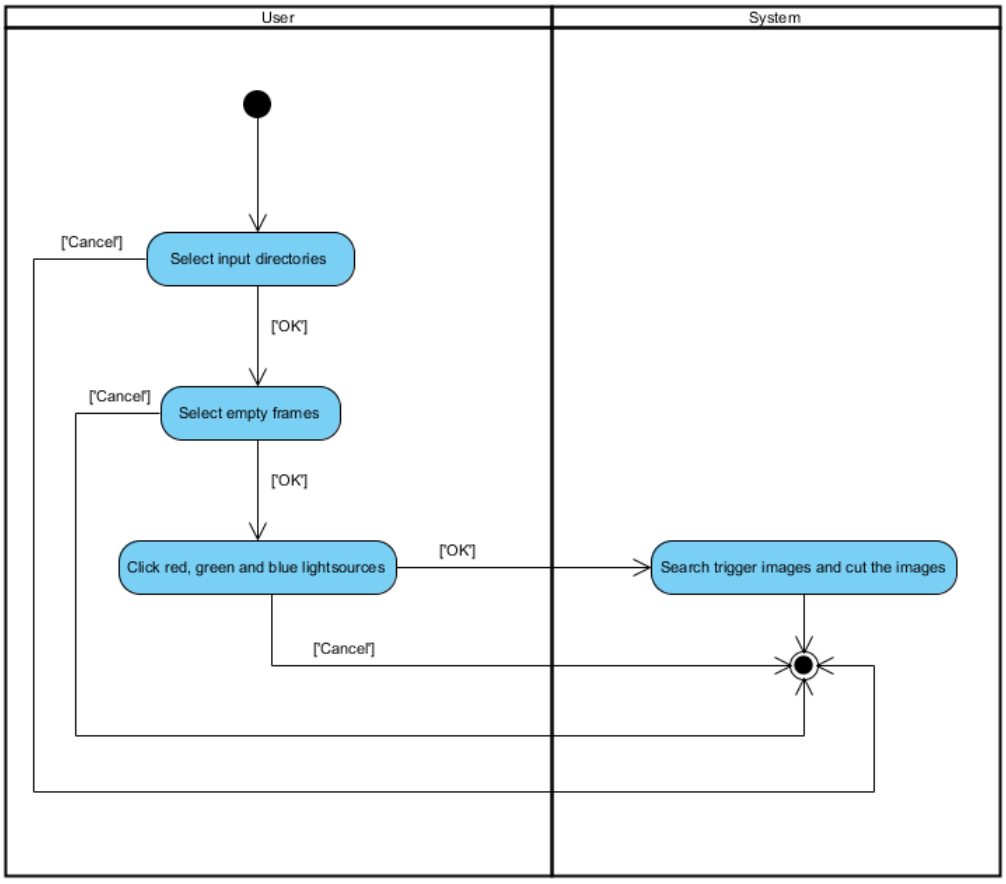

Fig. 4.14 Activity diagram for the process "Cut the sequence"

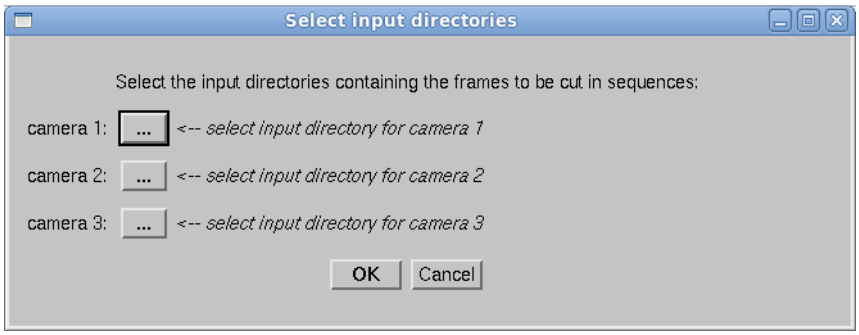

Fig. 4.15 Selection panel for the input directories

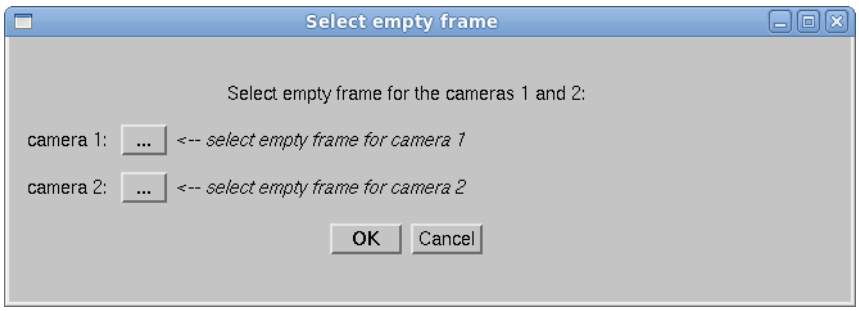

Fig. 4.16 Selection panel for the empty frame directores

The empty frame pictures are then shown and the user is asked to click on the red, green and blue lights. The process then starts and will take a while, as the program has to go through every picture. The application detects the areas with an increase of the scene brightness, which represent the trigger points where the images are separated. As they correspond to the point where the flash was fired, it will be the same for all of the three cameras. Therefore, the amount of pictures should be also the same for every camera, which is controlled by the program.

4.2.1.5. Light Source Normalization

As the assumption of having point light sources in photometric stereo can not be fulfilled, a light source normalization for correcting the uneven light distribution in the scene must be done.

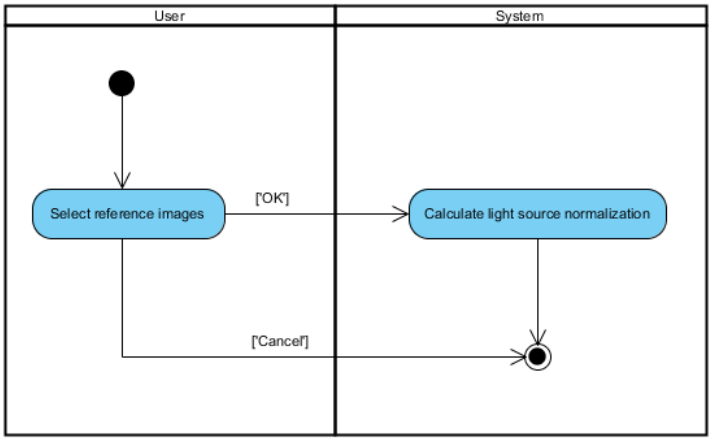

Fig. 4.17 Activity diagram for the process "Light source normalization"

As shown in Fig. 4.17, the user has to select the reference images (Fig. 4.18), that is the frames taken during the calibration, which are then used by the program to calculate the light source normalization.

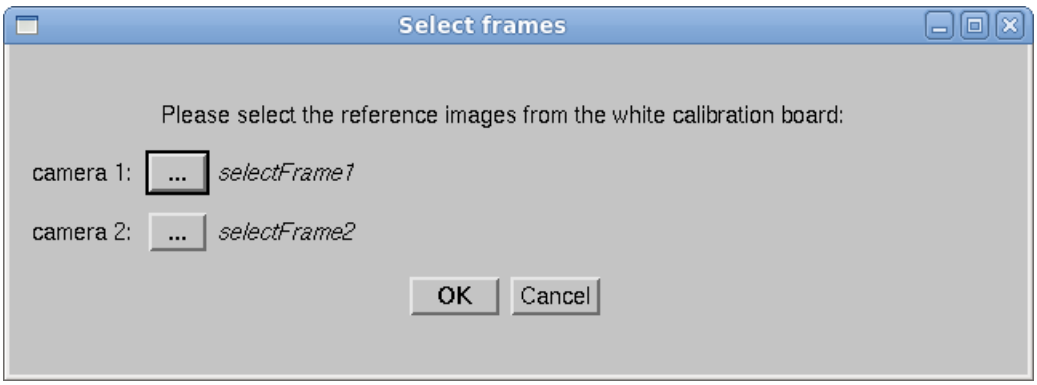

Fig. 4.18 Selection panel for the reference images

4.2.1.6. Mask Creation

The creation of the masks which is shown in Fig. 4.19 has undergone a few small adjustments since the implementation of Schroeder and Schulze in their thesis [34,35], which are described below.

For the mask creation, the user has to select the input directory of the frames he wants to make masks for and the output directory where they should be saved to (Fig. 4.20).

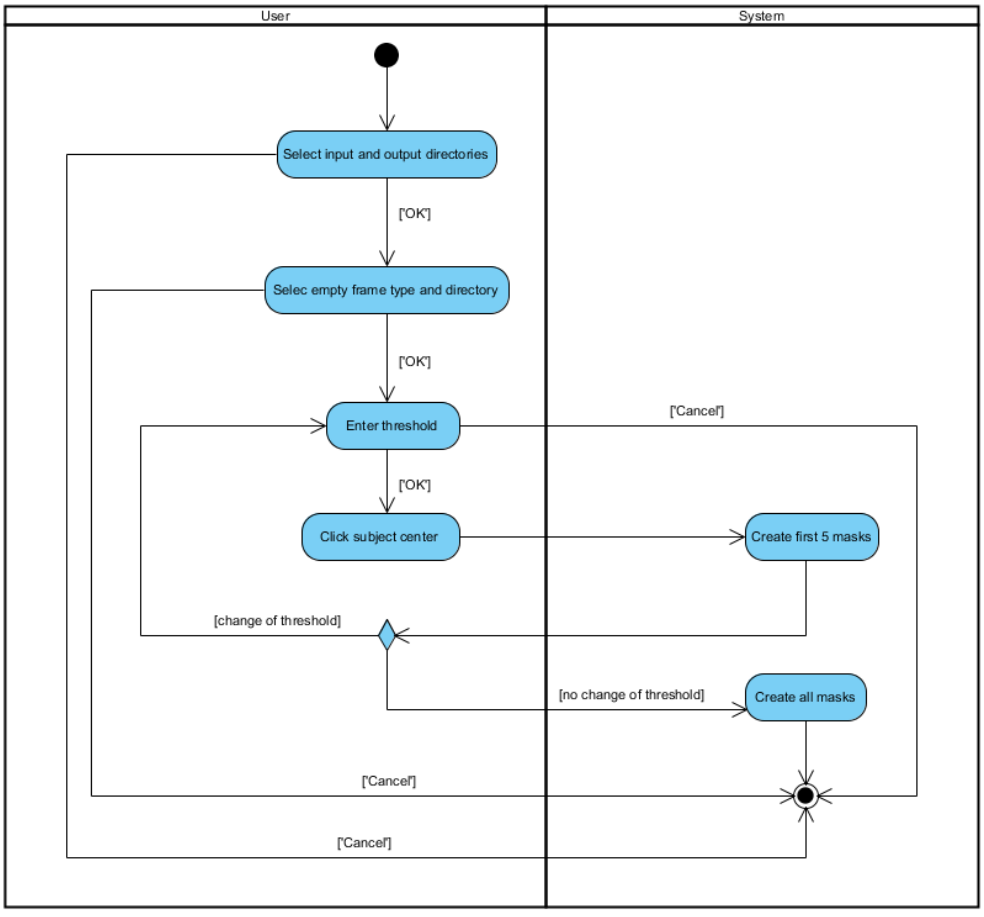

Fig. 4.19 Activity diagram for the process "Mask creation"

Fig. 4.20 Selection panel for input and output directories

After confirming the origin of the frames processed (from the profile camera or not), the type of empty frame to use has to be chosen: empty frame or whiteboard frame. Also, the file itself has to be indicated (Fig. 4.21).

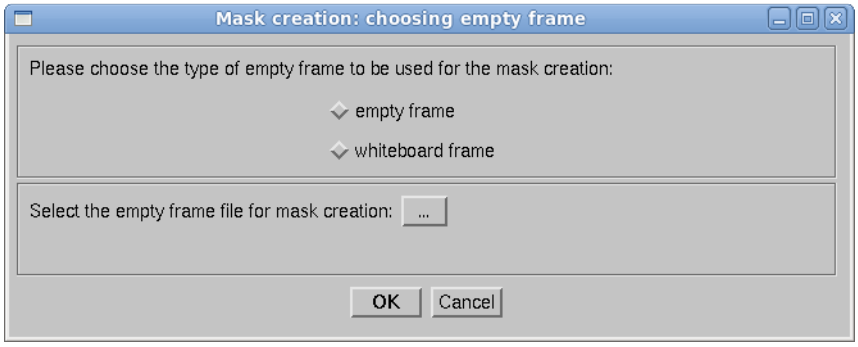

Fig. 4.21 Type of empty frame

The *empty frame* represents the picture of the empty exercise room with the same lighting conditions as the filmed subject, while the *whiteboard frame* corresponds to the image taken during the whiteboard calibration. The program then subtracts pixel by pixel the chosen frame from the frame which is just processed.

The main change in the mask creation was the handling of the threshold. Previously, its value was set to 0.9, representing the 90% quantile of the images' gray values [*35*]. As the quality of the masks was not continuously the same for every recorded situation, a more flexible value was desirable. This value was fixed and could only be changed by the programmer in the code. In order to fulfill different expectations of mask creation, a threshold with user interaction has been introduced.

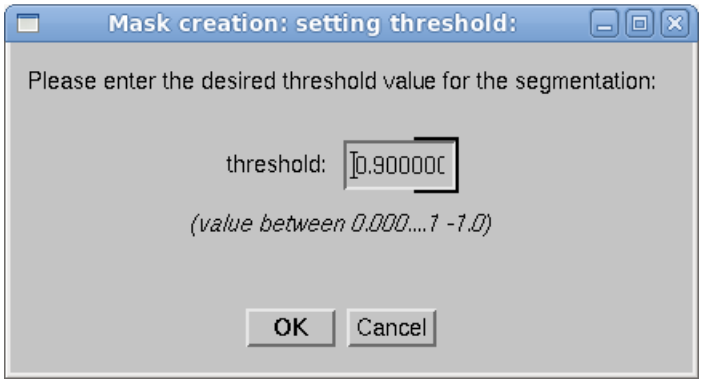

Fig. 4.22 Input panel for the threshold value

The user now has the possibility to enter the desired threshold value or to accept the default value of 0.9. After the user has clicked on the center of the subject, the program starts the mask creation for the first five masks which are shown on the desktop. After this run, the user can decide if the quality of the masks is good enough or if he wants to start the mask creation with another threshold value. If he decides to change the threshold, the masks created so far will be deleted and the process starts from the beginning. If he accepts the current masks, the process continues and the remaining masks are created without being shown at the desktop this time.

4.2.1.7. Patient Processing

As this process step wasn't working until the end of the project, neither the activity diagram can be created nor the user interaction can be explained.

4.2.1.8. Testing

The nesting of the different functions, especially of the graphical interface, made it very difficult to go through the steps of the different processes without losing track of the initial intention when trying out a certain program step. A further button has therefore been introduced to the starting panel for testing purposes. As there are some changes and improvements on the DynPS application that must be done, the button still appears when starting the program.

4.3. Perspectives and Research Areas for Further Work

As this work failed to improve the quality of the 3D reconstruction, it is indispensable to retain the points where the method can be developed in the future. This became the subject of the research at the end of the stay in Taiwan and the results are presented in the following sections.

4.3.1. Person Recruitment

The application DynPS is intended to be used in hospitals and with real patients. Schulze already achieved good 3D reconstruction with the dummy in his work [*35*] and began to test the method with real patients, but the results were not satisfying enough to be usable for hospital purposes. The technique therefore has to be improved, which can be done at several points.

For this purpose, an elaborate selection of patients and a good preparation is essential. This section will summarize the points which have to be taken care of when recruiting patient subjects.

Every individual presents some different attributes regarding the height, the weight, the fat distribution, the skin color, the belly button, the amount and size of moles, but also some kind of "irregularities" on the skin like the presence of cicatrices for example. All these characteristics have an impact on the quality of the 3D reconstruction and should be taken into account when selecting patient subjects.

Firstly, the method should be improved for average sized persons of both gender with rather white skin and normal weight. When the results for these patients are satisfying, then several groups of patients could be created, classifying the tested subjects regarding one attribute. As Schulze already tested some pregnant women in his thesis [*35*], the next step could be to continue his research. As the method could also be used for calculating the visceral fat measurement for diabetic patients, one group should certainly include a few subjects with overweight and/or different fat distribution. If the application yields good results at this moment, a next step could be to test some darker skinned persons. Also, a group of small persons and children is imaginable.

Schulze used two measures when dealing with real patient data [*35*]: the abdominal circumference in order to get some information about the shape of the subject's body, and the center of mass, which is assumed to have an evenly distributed mass in the whole body volume. The latter is a supposition which can't be fulfilled as it has been shown for pregnant women. Therefore, further research could be done in this field, too.

4.3.2. Approvals

The use of real patients leads to an important point when preparing the tests: the data privacy. One must keep in mind that the subjects are filmed for a few minutes with naked torso, in underwear or in tight white shirts. Not every person is probably aware of data privacy when being asked to act as a subject. So he or she should be informed how the procedure will be executed and what they have to expect. Also, a statement of agreement should be signed by the patients, declaring what will happen with the private data afterwards. If testing the procedure with children, the parents should also sign an agreement.

4.3.3. Weight and Shape Limitations

An interesting point would be to analyze if there are any limitations of the method regarding the weight of a person, the body shape and the fat distribution. This could be tested with a pregnant woman for example by taking videos in a regular interval during the whole pregnancy, or with highly obese persons.

4.3.4. Architectural Conditions

The whole method was developed and thought to be used in the rehabilitation department of the Wan Fang Hospital in Taipei, Taiwan. The light sources have been fixed on the ceiling of the therapeutic exercise room and haven't been moved since then. The whole setup of the video capture system has been built up for this place. Prof. Dr. Chen was the initiator of this research and is now the first contact person for it. As he is not working at the Wan Fang Hospital anymore, it will be important to clarify if some further research can still be done there or if a new place has to be found. In this case, the crucial point is to find a room with similar conditions as the previous exercise room where the system can be set up. If the place at disposal is restricted and if the setup which has been used so far (see "System Setup", 3.3.1) can't be kept, additional research has to be done on this field.

Besides that, the light sources have to be deinstalled at the Wan Fang Hospital and reinstalled in the new room. This will have the consequence that some new measurements and tests have to be carried out with the newly installed lighting system.

4.3.5. Time Requirement

The time which is required for the whole process was important in this work as the exercise room was occupied during the day for the patient treatments with the occupational therapists. The records had to be done at nighttime or on Sundays and therefore it was useful to know how long the measures would take. The time required will depend strongly on how many videos have to be taken and how much calibrations are needed. Also, when taking records of real patients, much more time will be needed as the subjects have to be instructed how the measure will take place. A good idea would be to give instructions the day before the video capture so that on the recording day the focus is set on the test.

The setup of the system is quite fast after the markers on the floor have been drawn. Most of the time is spent on adjusting the cameras no.1 and no.2 so that they are facing each other. Some more time will be require if the light sources do not illuminate one specific point and have to be corrected. Also, the measuring of the distances between the cameras and the whiteboard (or subject) needs a few moments.

The calibration however will take more time if different calibration spheres are tested. One must remember that every ball has to be fixed on the fourth tripod, which is getting more difficult with a bigger size of the sphere. Moreover, the ball has to be fixed on both sides of the calibration board so that it can be recorded by both of the front and backview cameras.

The video capture itself will take most of the time as the subjects have to change clothes, to be set in place and to move or be moved in the case of the dummy. Also if several subjects have to be filmed, some time will be needed for changing from one to the other.

Finally, the deinstallation of the system needs some more time, although it can be done quite quickly.

For this work, a normal capture session lasted for 2-3 hours depending on how many corrections had to be done and how many videos had to be taken. But for the first session, it is best to have a few hours so that the adaptations can be done without any need to hurry.

4.4. Requirements to the Staff Using the PS Method and DynPS

The use of the described method of Photometric stereo and the application DynPS requires some knowledge in order to get the best possible 3D reconstruction results and will be described in this section.

4.4.1. Required Knowledge

For this purpose, the user must imperatively get some basic information about the 3D Photometric Stereo which he will find in section 3.1.7. In addition, he should also read the section 3.3 where the whole process with its different steps is described. Before starting with the practical part of the work, the *Manual for Dynamic Photometric Stereo Application* (Schulze [*35*]) should be read meticulously.

After the successful recording, the video material has to be processed with the DynPS application. In order to get the best results of 3D reconstruction, the parameters in the program should be set correctly and the adequate files and directories must be chosen. This can only be reached when the user of the software is well-informed about the different process steps of the 3D reconstruction and how the substeps of the application work. Thus, the user should read the section 4.2.1 which describes the user interaction with the program.

4.4.2. Checklists

The material should be controlled in advance in order to ensure it is complete and in good condition, namely the following points:

- 6 light sources correctly adjusted, with working bulbs and cleaned dichroic filters
- 4 tripods
- 3 cameras with full batteries
- DV-tapes
- Flash unit
- Laser range finder
- Batteries for the flash unit and the laser range finder
- Whiteboard
- Calibration ball(s)
- Material for fixing the calibration ball on the 4^{th} tripod, if necessary
- Paper and pencil

The distances between the cameras and the subject/whiteboard should be measured with the laser range finder, as they are important parameters to be entered during the video processing with the DynPS application. The five distances to be determined are between:

- Cameras no. 1-3 and whiteboard
- Cameras no. 1-2 and calibration sphere

In order to have all the files required by the program, the user should ensure to film the following sequences:

- Empty frame (empty room with the same lighting conditions as the subject(s))
- Calibration ball(s)
- Subject(s)

5. Discussion

As no results can be discussed, this chapter will give some suggestions for further work on this research. The crucial points for continuing the present work will be explained briefly.

5.1. Crucial Points for Takeover

This work was intended to improve the 3D reconstruction of real patients, but unfortunately presented some technical and personal obstacles (section 4.1), so that this goal couldn't be reached. Therefore, it is necessary to document the crux of the matter in case this work will be continued by someone else. This is the main goal of this section.

5.1.1. Up-to-date Code Files

First of all, the actuality of the code should be checked. For this work, an older version of the code files was provided, which didn't correspond to the newest one. Unfortunately, this came out at the end of the stay in Taiwan, so that the work done so far couldn't be undone and the code has already been transformed when improving the graphical user interface. Therefore, the code files of this work and the newest version of Schulze [*35*] should be compared, replaced and corrected when necessary. The goal should be to have the current version of the application logic of Schulze and the graphical user interface of this work.

5.1.2. DynPS

After the program code has been corrected, improvements can be done at the application itself as described by the following sections.

5.1.2.1. Masking

The masking process can be improved at different points. The mask creation for the front and back camera should be examined with real patient data as this was only partly possible during this work. Then the mask creation could be improved by introducing a variable threshold for the side camera as it has been introduced for the front and back cameras.

5.1.2.2. Patient Processing

As soon as the process of mask creation is working well, the main task is to make the patient processing running. This was not possible during this work because of the different problems described in section 4.1. The main task will be to improve the 3D reconstruction by comparing different pictures. For this, different white shirts can be tested on the patients to figure out which generates the best reconstructions. Besides that, an emphasis should be put on the calibration of the system. By using different calibration spheres, the calibration could be improved so that also the reconstruction at the end of the process will be of a better quality.

When these two tasks are finished, the method should be applied to different real patients as already seen in section 4.3.1. Several captures should be taken for each type of person, so that the results can be compared and further improvements considered.

5.1.3. System Setup

A very important point if taking over this work is the system setup. The previous work has been done in the therapeutic exercise room where the six lamps have been fixed on the ceiling. A part of the system was therefore not removable. As Prof. Dr. Chen is not working at the Wan Fang Hospital anymore, a solution for the system setup has to be found. The easiest one would be to set up the system at the same place, so that the material does not have to be moved. This has to be clarified with the responsible persons at the Wan Fang Hospital. The other possibility would be to set up the system in another room. For this, an appropriate place must be found where the six lights can be fixed at the ceiling and the place for setting up the whole system is big enough. Moreover, it should be clarified if the room is needed by other persons or if it could be used just for this purpose.

When looking for a new room, one should keep in mind that it should either have no windows or it should be possible to darken the room during the tests. Also, the door should be lockable as the camera and lighting material used is expensive.

5.1.4. Patient Recruitment

A patient recruitment described in section 4.3.1 which is done carefully will most likely yield the best 3D reconstruction results possible. Therefore, the planning of the captures themselves should be done conscientiously, in order to guarantee a smooth execution of the different processes on the experiment day.

5.1.5. Support

One of the most crucial points of this work was the lack of the support needed and the communication between the different persons involved. When taking over this project, the candidate should clarify in advance the responsibility and competence of every participant. The advisor in Taiwan should become aware of his or her responsibility when an exchange student takes over the project. A sufficient amount of time should be available for the support of the work. The responsible supporter in Germany should control the current state of the work from time to time and react consequently when necessary. On the other hand, exchange students themselves have to report to both sides where they stand and which difficulties they encountered during their work.

5.1.6. Preparation Needed for Future Candidates

In order not to repeat a situation similar to this work, there are some points a future candidate should know or fulfill.

A good knowledge of the operating system Linux and the work with the command line is essential as the program is intended to be used on Linux. When the candidate prefers to work on Windows, he should previously install the necessary software described in section 3.2.3. and guarantee the accessibility to Linux. Also, he should learn the basics about Photometric Stereo. Besides that, getting first impression of the program by trying it out would be recommendable.

6. Conclusion and Perspective

The intention of this work was to improve the method of volume reconstruction presented by Schroeder and Schulze [34,35] on different levels. By comparing real patient data with several calibration spheres, a statement could have been made about the best calibration setting. The use of white shirts on the subjects could have corrected the distortions due to skin irregularities. Besides that, the patient data of persons with different characteristics could have helped to make predictions about the improvements to do in the program for getting the best 3D reconstruction quality. Finally, a more convenient graphical user interface was the main goal for making the use of the application more simple to non-technical staff.

All these points could have been reached by having a better communication between the project participants as there were a lot of misunderstandings leading at the end to a lot of time loss. The technical problems happening were unpredictable but also led to an important delay. Also, a better preparation on every side would have been advisable to have more time to focus on the essential work.

Finally, the emphasis of this work had to be changed due to the circumstances. The graphical user interface has been completed and changed in order to make the program flow more understandable for the users. Also, the information for a potential takeover for further students have been collected.

The main goal of this work couldn't be reached for the different reasons mentioned in section 4.1. However, the project could be taken over by another student in the context of a further student exchange between the Taipei Medical University and the University of Heidelberg/Heilbronn University. The obstacle then is to find a solution where to setup the system as Chi-Hsien Chen doesn't work at the Wan Fang Hospital anymore. With the agreement of the Department of rehabilitation of the hospital and with a good organization, it is imaginable to continue the work at the same place. Either way, a good planning and above all an intensive communication is needed if further research should be done on this project.

References

1. Alldrin, N., Zickler, T. and Kriegman, D. *Photometric Stereo With Non-Parametric and Spatially-Varying Reflectance*. in *IEEE Conference on Computer Vision and Pattern Recognition (CVPR)* (Anchorage, Alaska, USA 2008).
2. Barsky, S. and Petrou, M. *The 4-Source Photometric Stereo Technique for Three-Dimensional Surfaces in the Presence of Highlights and Shadows*. IEEE Transactions on Pattern Analysis and Machine Intelligence 24(2003).
3. Basri, R., Jacobs, D. and Kemelmacher, I. *Photometric Stereo with General, Unknown Lighting*. International Journal of Computer Vision 72, 239-257 (2007).
4. Christensen, P.H. and Shapiro, L.G. *Three-dimensional shape from color photometric stereo*. International Journal of Computer Vision 13, 213-227 (1994).
5. Coleman, E.N. and Jain, R. *Obtaining 3-Dimensional Shape of Textured and Specular Surfaces Using Four-Source Photometry*. Computer Vision, Graphics and Image Processings 18, 309-328 (1982).
6. Davidovits, P. *Physics in Biology and Medicine*, (Elsevier, 2008).
7. Dedolight. *Dedolight catalog*. (2007).
8. Drbohlav, O. and Chantler, M. *On Optimal Light Configurations in Photometric Stereo*. in *10th IEEE International Conference on Computer Vision*, Vol. 2 1707-1712 (Beijing, China, 2005).
9. Frankot, R.T. and Chellappa, R. *A Method for Enforcing Integrability in Shape from Shading Algorithms*. IEEE Transactions on Pattern Analysis and Machine Intelligence 10(1988).
10. Georgieva, L., Dimitrova, T. and Angelov, N. *RGB and HSV colour models in colour identification of digital traumas images*. in *International Conference on Computer Systems and Technologies* (2005).
11. Harten, H.-U. *Physik für Mediziner*, (Springer Verlag, 2007).
12. Hawkes, P.W. *Advances in imaging and electron physics*, (Academic Press, ELSEVIER, 2009).
13. Hayakawa, H. *Photometric stereo under a light source with arbitrary motion*. J. Opt. Soc. Am. A 11(1994).
14. Hernandez, C., Vogiatzis, G. and Cipolla, R. *Multi-view photometric stereo*. Pattern Analysis and Machine Intelligence, IEEE Transactions 30, 548-554 (2008).
15. Hernandez, C. and Vogiatzis, G. *Shape from Photographs: A Multi-view Stereo Pipeline*, (Springer-Verlag, 2010).
16. Hertzmann, A. and Seitz, S.M. *Example-Based Photometric Stereo: Shape Reconstruction with General, Varying BRDFs*. IEEE Transactions on Pattern Analysis and Machine Intelligence 27, 1254-1264 (2005).
17. Horn, B.K.P. and Sjoberg, R.W. *Calculating the reflectance map*. Applied Optics 18, 1770-1779 (1978).
18. Horn, B.K.P., Woodham, R.J. and Silver, W.M. *Determining shape and reflectance using multiple images*. MIT AI Memo-490 (1978).
19. Horn, B.K.P. *Hill Shading and the Reflectance Map*. in *Proc.of the IEEE*, Vol. 69, No. 1 (1981).
20. Horn, B.K.P. *Height and gradient from shading*. International Journal of Computer Vision 5 37-75 (1990).
21. Horovitz, I. and Kiryati, N. *Depth from Gradient Fields and Control Points: Bias Correction in Photometric Stereo*. Image and Vision Computing 22, 681-694 (2004).
22. Klette, R. and Schlüns, K. *Height data from gradient fields*. Proc. Machine Vision Applications, Architectures, and Systems Integration 5, 204-215 (1996).
23. Lee, S.-W., Wang, P.S.P., Yanushkevich, S.N. and Lee, S.-W. *Noniterative 3D face reconstruction based on photometric stereo*. International Journal of Pattern Recognition and Artificial Intelligence 22, 389-410 (2008).
24. Manfrotto. *Manfrotto Shop*.
25. Masero, V., Leon-Rojas, J.M. and Moreno, J. *Volume Reconstruction for Health Care - A Survey of Computational Methods*. Annals of the New York Academy of Sciences, 198-211 (2002).

26. Nayar, S.K., Ikeuchi, K. and Kanade, T. *Determining Shape and Reflectance of Hybrid Surfaces by Photometric Sampling*. IEEE Transactions on Robotics and Automation 6, 418-431 (1990).
27. Nicodemus, F.E., Richmond, J.C. and Hsia, J.J. *Directional Reflectance and Emissivity of an Opaque Surface*. Institute for Basic Standards, National Bureau of Standards, Washington D.C. (1977).
28. Oren, M. and Nayar, S.K. *Generalization of Lambert's Reflectance Model*. in *Proc. of the 21st annual conference on Computer graphics and interactive techniques* (1994).
29. Plata, C., Nieves, J.L., Valero, E.M. and Romero, J. *Trichromatic red-green-blue camera used for the recovery of albedo and reflectance of rough-textured surfaces under different illumination conditions*. Applied Optics 48, 3643-3653 (2009).
30. Plataniotis, K.N. and Venetsanopoulos, A.N. *Color Image Processing and Applications*, (Springer Verlag, 2000).
31. Press, W.H., Teukolsky, S.A., Vetterling, W.T. and Flannery, B.P. *Numerical Recipes in C: The Art of Scientific Computing*, (Cambridge University Press, 1992).
32. ROSCO. *The ROSCO guide to color filters*. ((downloaded in 2011)).
33. Schroeder, W. *Three-Channel Dynamic Photometric Stereo - A New Method for 4D Surface Reconstruction*. University of Heidelberg (2008).
34. Schroeder, W., Schulze, W., Wetter, T. and Chen, C.-H. *Three-channel dynamic photometric stereo: A new method for 4D surface reconstruction and volume recovery*. Proc. SPIE, Proc. 7072(2008).
35. Schulze, W. *Three Channel Dynamic Photometric Stereo - Application on Human Body Surface Recovery, Volume Measurement and Movement Analysis*. University of Heidelberg (2008).
36. Serway, R. and Jewett, J. *Physics for Scientists and Engineers*, (Brooks / Cole, 2010).
37. Smith, M. and Smith, L. *Dynamic photometric stereo—a new technique for moving surface analysis*. Image and Vision Computing 23, 841-852 (2005).
38. Spence, A.D. and Chantler, M.J. *Optimal illumination for three-image photometric stereo using sensitivity analysis*. IEE Proc.-Vis. Image Signal Process., Vol. 153, No. 2, April 2006 153, 149-159 (2006).
39. TaiwanHealthCare. *Wan Fang Hospital*. (2011).
40. Treleaven, P. and Wells, J. *3D Body Scanning and Healthcare Applications*. Computer 40, 28-34 (2007).
41. Trussell, H.J., Saber, E. and Vrhel, M. *Color Image Processing*. IEEE Signal Processing Magazine 22, 14-22 (2005).
42. Wei, T. and Klette, R. *On Depth Recovery from Gradient Vector Fields*. Vol. 203 (ed. Report, C.a.I.T.R.T.) (2007).
43. Wolff, L.B., Nayar, S.K. and Oren, M. *Improved Diffuse Reflection Models for Computer Vision*. International Journal of Computer Vision 39, 55-71 (1998).
44. Woodham, R.J. *Reflectance Map Techniques for Analyzing Surface Defects in Metal Castings*. Massachusetts Institute of Technology (1977).
45. Woodham, R.J. *Photometric method for determining surface orientation from multiple images*. Optical Engineering 19, 139-144 (1980).
46. Wu, Z. and Li, L. *A Line-Integration Based Method for Depth Recovery*. Computer Vision, Graphics and Image Processings 4, 53-66 (1988).
47. Yaroslavsky, L.P., Moreno, A. and Campos, J. *Frequency responses and resolving power of numerical integration of sampled data*. Optics Express 13, 2892-2905 (2005).
48. Zheng, Z., Ma, L., Li, Z. and Chen, Z. *An extended photometric stereo algorithm for recovering specular object shape and its reflectance properties* Computer Science and Information Systems (ComSIS) 7, 1-12 (2010).

Figure list

Appendix

Events in ps3dcontrol_event.pro

Overview of the event handling in the application DynPS

1. ***grab***

Pop-ups: enter

- ***ok_grab***
  set video duration in duration

2. ***extract***

Pop-ups: select2, rename

- ***select***
  - ***selectVideodir***
    set video directory for frame extraction in videodirExtract
  - ***selectFramedir***
    set frame directory for frame extraction in framedirExtract
  - ***selectRenamefile***
    select the path of the file to rename in oldPath
  - ***rename***
    set the path of the new filename in newPath

3. ***lsmatrix***

Pop-ups: select2, distances, okcancel

- ***select***
  - ***selectCalfile1***
    set calibration file for camera 1 in calfile1
  - ***selectCalfile2***
    set calibration file for camera 2 in calfile2
- ***ok_distances***
  set distances between whiteboard/ball and camera in:
  wb_cam1, wb_cam2, wb_cam3, ball_cam1, ball_cam2
- ***ok_destroy***
  destroys the pop-up

4. ***cut***

Pop-ups: select3, select2, okcancel

- ***ok_destroy***
  destroys the pop-up
- ***select***
  - ***cut1***
    set input directory for camera 1 in indirCut1
  - ***cut2***
    set input directory for camera 2 in indirCut2
  - ***cut3***
    set input directory for camera 3 in indirCut3
  - ***emptyFrame1***
    set empty frame for camera 1 in eframe1
  - ***emptyFrame2***
    set empty frame for camera 2 in eframe2

5. normcalib

Pop-ups: select2

- ***select***
  - ***selectRefimg1***
    set reference image (from whiteboard) for camera 1 in refImg1
  - ***selectRefimg2***
    set reference image (from whiteboard) for camera 2 in refImg2

6. ***masking***

Pop-ups: select2, choice, thresh, thresh2

- ***select***
  - ***selectIndirMask***
    set input directory in indirMask
  - ***selectOutdirMask***
    set output directory in outdirMask
- ***ok_destroy***
  destroys the pop-up
- ***ok_thresh***
  set threshold in thresh
- ***ok_thresh2***
  set horizontal threshold in threshhor and vertical threshold in threshver
- ***eframeMask***
  set the empty frame in eframeMask

7. ***process***
   Pop-ups: select7, okcancel
   - process_select
     - ***pro1***
       set frames input directory for camera 1 in infront
     - ***pro2***
       set mask input directory for camera 1 in maskfront
     - ***pro3***
       set frames input directory for camera 2 in inback
     - ***pro4***
       set mask input directory for camera 2 in maskback
     - ***pro5***
       set frames input directory for camera 3 in prof
     - ***pro6***
       set mask input directory for camera 3 in maskprof
     - ***pro7***
       set directory for storing results in storedir
   - ***ok_destroy***
     destroys the pop-up

8. ***exit***
   Exits the program
9. ***test***
   For testing purposes